TM-

TECHNICAL MEMORANDUM

TWO FLUID MODEL FOR THERMAL STRATIFICATION IN THE APOLLO CRYOGENIC OXYGEN TANKS

Bellcomm

BELLCOMM, INC.
955 L'ENFANT PLAZA NORTH, S.W., WASHINGTON, D.C. 20024

COVER SHEET FOR TECHNICAL MEMORANDUM

TITLE- Two Fluid Model for Thermal Stratification in the Apollo Cryogenic Oxygen Tanks

TM-71-2031-2

FILING CASE NO(S)- 320

DATE- October 22, 1971

AUTHOR(S)- J. A. Saxton

FILING SUBJECT(S) (ASSIGNED BY AUTHOR(S))-

ABSTRACT

The rate of thermal energy transfer by natural convection from a solid heating element to a receiving fluid is significantly reduced in the low acceleration conditions of space flight. In the Apollo cryogenic oxygen tanks the effect of reduced natural convection is compounded by the low thermal conductivity of oxygen and the low level of thermal radiation at the temperatures of tank operation. As a result, regions of differing temperature develop within the oxygen; this is termed thermal stratification. Flight experience and thermodynamic analysis has shown that substantial pressure drops can result from sudden mixing of thermally stratified oxygen. Fans were provided to control stratification on the initial Apollo flights. The fans were removed as one of the safety precautions taken following the oxygen tank failure on Apollo 13. This paper describes one of a number of investigations conducted to insure a sufficient understanding of tank operation without the destratification fans.

It is observed on Apollo flights that for oxygen densities greater than 42 lb/ft^3 the heater operation time to achieve a desired pressure rise is half that which would be required if the energy were uniformly dispersed. A two fluid model was developed to describe this effect of stratification on the tank's pressurization behavior. The model attributes the increase in pressure rise rate to compression of the bulk fluid in response to expansion of the heated fluid adjacent to the heater. The model assumes that during the heating operation the adjacent fluid retains nearly all the heater energy and has no mass interaction with the bulk fluid. The hot fluid temperatures predicted by the model are in reasonable correspondence with the observed heater temperatures. The model indicates that the fraction of the fluid interacting with the heater increases with decreasing density, from less than 0.1% at full tank to roughly 1% at 50% quantity, the lowest quantity at which stratification effects on pressure are observed.

DISTRIBUTION

COMPLETE MEMORANDUM TO

CORRESPONDENCE FILES:

OFFICIAL FILE COPY
plus one white copy for each additional case referenced

TECHNICAL LIBRARY (4)

NASA Headquarters

J. Allman/MAE
C. H. King/MAE
A. S. Lyman/MAP
R. A. Petrone/MA
J. F. Saunders/MAE
W. E. Stoney/MAE

MSC

P. F. Cantin/FM7
W. A. Chandler/EA5
E. Chimenti/ES55
A. W. Joslyn/PD7
F. Plauche/EP5
R. R. Rice/EP5
W. E. Rice/EP5
R. C. Ried/ES5
W. Scott/FM7
W. E. Simon/EP5
J. Smithson/EP5

NASA, Langley

J. T. Suttles

NASA, Ames

B. S. Baldwin

Boeing, Washington

J. Mulcahy

Boeing, Houston

C. K. Forester
H. W. Patterson
R. Reysa
D. D. Rule

North American Rockwell

I. M. Chen
W. L. Owens

National Bureau of Standards, Boulder

R. H. Kropschot

Lockheed

J. Williams

TRW, Houston

R. A. Cailleteau
P. J. Heinmiller
W. E. Piske
R. K. M. Seto

Georgia Tech

W. Wulff
N. Zuber

Distribution List (Cont.)

Bellcomm

G. M. Anderson
D. O. Baechler
A. P. Boysen, Jr.
J. P. Downs*
R. Gorman
D. R. Hagner
J. J. Hibbert
W. W. Hough
R. N. Kostoff
H. S. London
D. Macchia
J. Z. Menard
I. M. Ross*
J. A. Schelke
P. F. Sennewald
L. D. Sortland
W. Strack
V. Thuraisamy
J. W. Timko*
R. L. Wagner
M. P. Wilson*
All Members of Department 2031
Department 1024 File

*Abstract Only

TABLE OF CONTENTS

Bellcomm

955 L'Enfant Plaza North, S.W.
Washington, D. C. 20024

date: October 22, 1971

to: Distribution

from: J. A. Saxton

TM-71-2031-2

subject: Two Fluid Model for Thermal Stratification in the Apollo Cryogenic Oxygen Tanks - Case 320

TECHNICAL MEMORANDUM

INTRODUCTION

The physical situation considered here is the transfer of thermal energy from a solid heating device to a contained fluid in order to maintain container pressure as fluid is withdrawn. Convection, natural or forced, usually acts as the principal mode for such solid-to-liquid thermal energy transfer, with radiation and conduction playing a secondary role. In the case of nonpropulsive space flight, however, the acceleration driving force for natural convection is greatly reduced.* In this case, unless a means of forced convection is provided, it may not be possible to efficiently transfer energy from the heating device to receiving fluid. Fluid pockets of different temperatures may buildup. The existence of such temperature nonuniformities within a fluid otherwise in thermodynamic equilibrium is termed thermal stratification. When a thermally stratified fluid is suddenly mixed, as by a spacecraft propulsive maneuver, the resulting pressure may lie considerably below its unmixed value.** Such sudden drops of pressure are termed pressure decays. They have been observed on both Gemini and Apollo flights.

This paper considers the nature of thermal stratification and the evidence of its occurrence in the Apollo cryogenic oxygen tanks. These tanks supply oxygen

---

*The acceleration forces during the earth-lunar coast portions of Apollo flights are less than 10^{-5} earth gravity except during propulsive vehicle maneuvers.

**It can be shown thermodynamically that the pressure resulting from mixing a thermally stratified fluid can be less than or equal to its original value, but never greater.

for crew breathing and fuel cell operation. The oxygen is maintained above its critical pressure to provide a single fluid phase for accuracy in quantity gauging and uniformity in fluid outflow. A cylindrical heater along the tank's centerline supplies the energy needed to sustain tank pressure. On Apollo 13 and prior Apollo flights, fans located at the top and bottom of the heater tube were operated periodically to alleviate temperature nonuniformities. These fans were removed, however, as one of the protective steps taken following the failure of the Apollo 13 oxygen tanks. As a result, Apollo 14 was the first Apollo flight without a direct method for control of thermal stratification.

To insure that there was a sufficient understanding of the potential effects of noncontrolled stratification, an Apollo Cryogenic Oxygen Tank Analysis Team was formed. The work discussed in this paper represents one facet of the effort of the Analysis Team.* A two fluid model is developed to describe the effect of stratification on pressure behavior and is used with flight data to estimate how much fluid interacts with the heater during each cycle. The flight data analyzed is primarily from Apollo 14, which had improved instrumentation and more complete data coverage. Supplementary information on the tanks and their operation; the appropriate thermodynamic expressions describing pressure, energy, and mass variations; the development of the two fluid equations; and representative calculations are included in the Appendices.

I. THERMAL STRATIFICATION IN THE APOLLO OXYGEN TANKS

A. Thermal Stratification in Oxygen

Oxygen is particularly susceptible to stratification in the absence of convection in that it is a very poor conductor, equivalent to cork board. Also, at the relatively low temperatures of Apollo tank and heater operation there is little radiated energy. For the conditions corresponding to tank quantities of 50% and above, the heater radiates energy at less than 10 Btu/hr, as compared to a total heater power of 375 Btu/hr. The energy radiated from the heater passes directly to the tank wall, since oxygen is essentially transparent to infrared radiation (2). The energy is subsequently transferred

---

*Other aspects are described in papers presented at the symposium serving as the final meeting of the Team (1).

from the wall to the oxygen by conduction and convection. It can be treated as a supplement to the heat leak entering the tank from the surrounding environment.

Because conduction and radiation are inefficient heat transfer modes in oxygen, steep temperature gradients develop in the very low convection conditions of the non-propulsive portions of the Apollo flights. The specific nature of these gradients has been the subject of a number of investigations (3, 4, 5, 6). This investigation concentrates on the pressure effects of stratification, and uses pressure data to determine a mean temperature for the hot fluid adjacent to the heater.

B. Effect on Pressurization Behavior

At high fluid densities, pressure variations with time furnish a sensitive indication of stratification. The reason for this is as follows. The fluid is at uniform pressure throughout. Therefore, the regions of higher temperature have lower density. The related thermal expansion of the heated fluid exerts a compressive force on the remaining fluid. At high fluid densities it is observed that significantly less energy is required to achieve a given pressure rise under these conditions than if the heat were distributed uniformly. As a result, the heater on-times are shorter in the presence of stratification. Following heater deactivation, heat transfer tends to dissipate the high temperature regions, thus reducing the artificially high pressure achieved. The pressure decline from heat transfer combines with the natural pressure loss accompanying mass outflow. The two effects together cause a more rapid pressure drop and shorter heater off-time than if stratification had not occurred. Thus, the occurrence of more frequent, shorter heater cycles than predicted from uniform heat transfer serves to indicate the presence of stratification.

In the Apollo tanks there is continuous mass withdrawal, with intermittent heater operation. Tank flexibility leads to a small but significant volume expansion with increasing pressure. The first law of thermodynamics has been rearranged in Appendix B into a form appropriate for these conditions. The resulting expression is:

$$\dot{p} = \frac{\phi}{V} \left(Q - \rho \Theta \dot{V} - \Theta \omega \right) \qquad (1)$$

Here $\dot{p}$ is the rate of pressure change with thermal energy input rate Q, volume expansion rate $\dot{V}$, and mass outflow rate ω. The parameters:

$$\phi \equiv \frac{1}{\rho}\left(\frac{\partial p}{\partial u}\right)_{\rho} \tag{2}$$

and

$$\Theta \equiv -\rho\left(\frac{\partial h}{\partial \rho}\right)_{h} \tag{3}$$

are thermodynamic state variables arising from this arrangement of the first law. Their variation with density is shown in Figure 1 (7). ρ, u, h, and V are the fluid density, internal energy, enthalpy, and volume.

The ability through stratification to pressurize the tank with less energy than required if the heat were distributed uniformly renders the tank subject to sudden pressure decays upon tank agitation, as in a vehicle maneuver. At the high bulk densities associated with the early phases of the mission the potential for pressure decay increases cumulatively if a number of heating cycles occur while the tank mixing is minimal, such as in attitude hold. The largest pressure decay yet observed was a 145 psi drop on Apollo 12.* There was concern prior to flight that Apollo 14 might encounter larger pressure decays due to the removal of the destratification fans.

C. Occurrence on Apollo

Apollo 14 heater data are plotted as a function of tank quantity in Figure 3. The heater on-times necessary to raise the tank pressure from its lower operating limit to upper limit are shown as a function of oxygen quantity in the tank. 100% quantity corresponds to 330 lbs. and 0% to 6.6 lbs., the residual remaining at ambient conditions. For the 4.76 ft^3 tanks, the quantities can be equivalently expressed as densities of 69.5 and 1.39 lb/ft^3, respectively.

---

*Figure 2 shows a typical pressure decay following a fan cycle on Apollo 12. The deltas, Δ and δ, indicate the deviations between stratified and uniform heating and cooling rates for the heating cycle preceding fan operation.

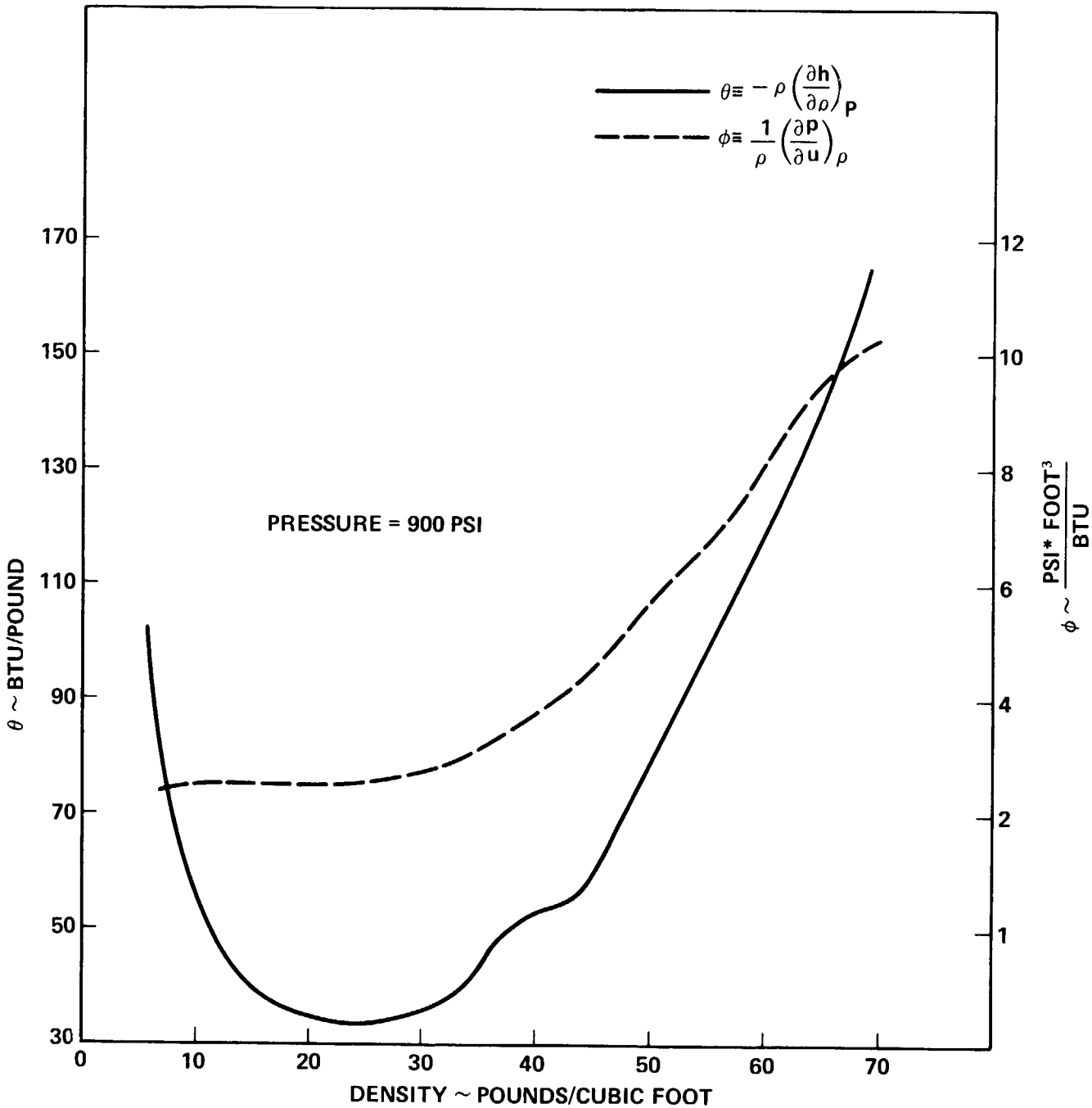

FIGURE 1 - PHI AND THETA FOR OXYGEN

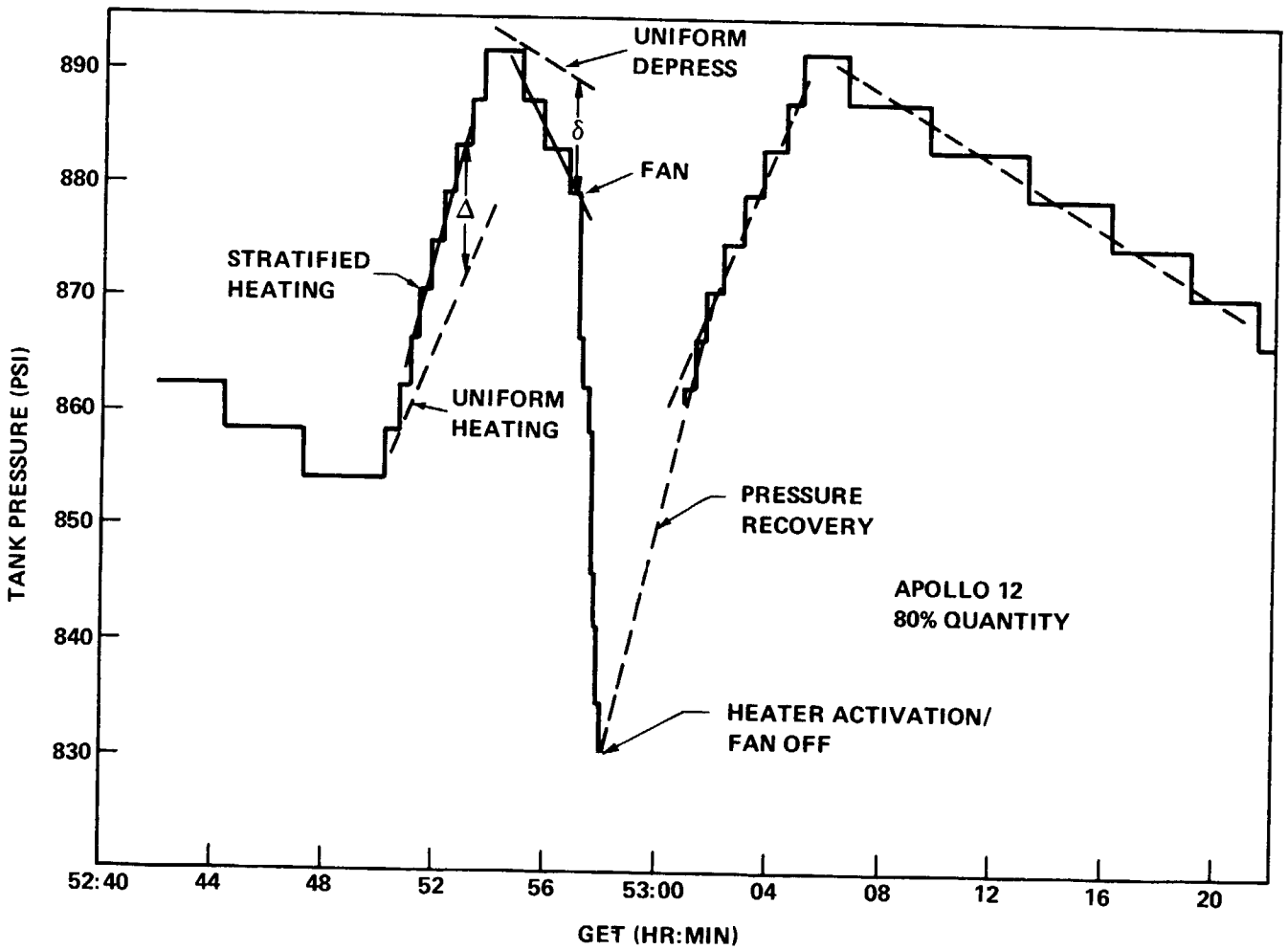

FIGURE 2 - PRESSURE DECAY FOLLOWING FAN CYCLE

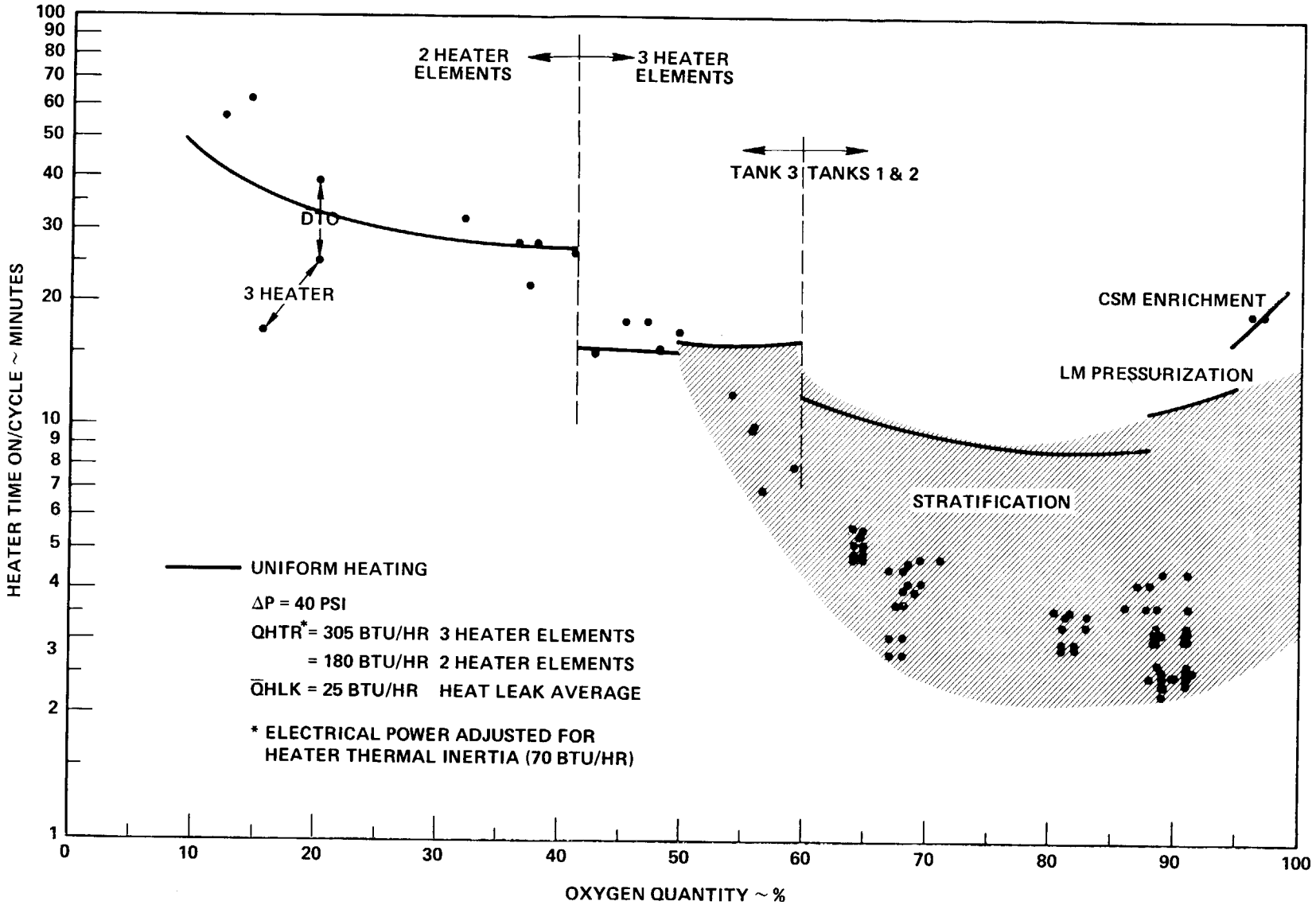

FIGURE 3 - APOLLO 14 PRESSURIZATION TIMES DEPICTING EFFECT OF STRATIFICATION

The data above 60% are from Tanks 1 and 2 whose heaters were operated concurrently, and the data below 60% are from Tank 3 which was operated in a single tank mode. (The philosophy of tank usage is discussed in Appendix A.) In order to offset high heater temperatures at lower quantities, the Tank 3 heater was operated with only two of its three heater elements below 41%. This reduced its energy input rate from 375 to 250 Btu/hr, and consequently led to longer heater cycles at the lower quantities.

The pressure rise times predicted for uniform heating are also shown in Figure 3. The segmented nature of the uniform heating curve is due to the variations in mass outflow during the mission. The mass outflow rates are plotted as a function of quantity in Figure 4. Since Tank 3 operates in a single tank mode, its flowrates are significantly higher than those from Tanks 1 and 2.

Examining Figure 3 we see that above 50% the pressure rise times are noticeably less than required for uniform heating. And above 60% the observed times are roughly one-half the uniform heating times. Clearly then there was stratification in the cryogenic tanks on Apollo 14.

It is of interest to see whether the destratification fans on Apollo 12 eliminated stratification. The fans were used twice each day to stir the tank contents. The mass flowrates from each of the two tanks on Apollo 12 were relatively uniform, with a mean flow of 1 lb/hr. Figure 5 shows the pressure rise data for Apollo 12 compared with the predictions for uniform heating. Apparently, the destratification fans did not eliminate stratification.

The presence of stratification enables the oxygen tanks to operate for a number of heating cycles with an energy deficit. Eventually, however, a propulsive maneuver mixes the tank contents, and the energy deficit must be replenished. Thus, the net energy supplied to the tank over an extended time period must be sufficient to support tank outflow irrespective of short term stratification. Since in a sequence of pressure cycles there is no net pressure change or tank volume change, Equation (1) becomes:

$$Q = \theta\omega \qquad (4)$$

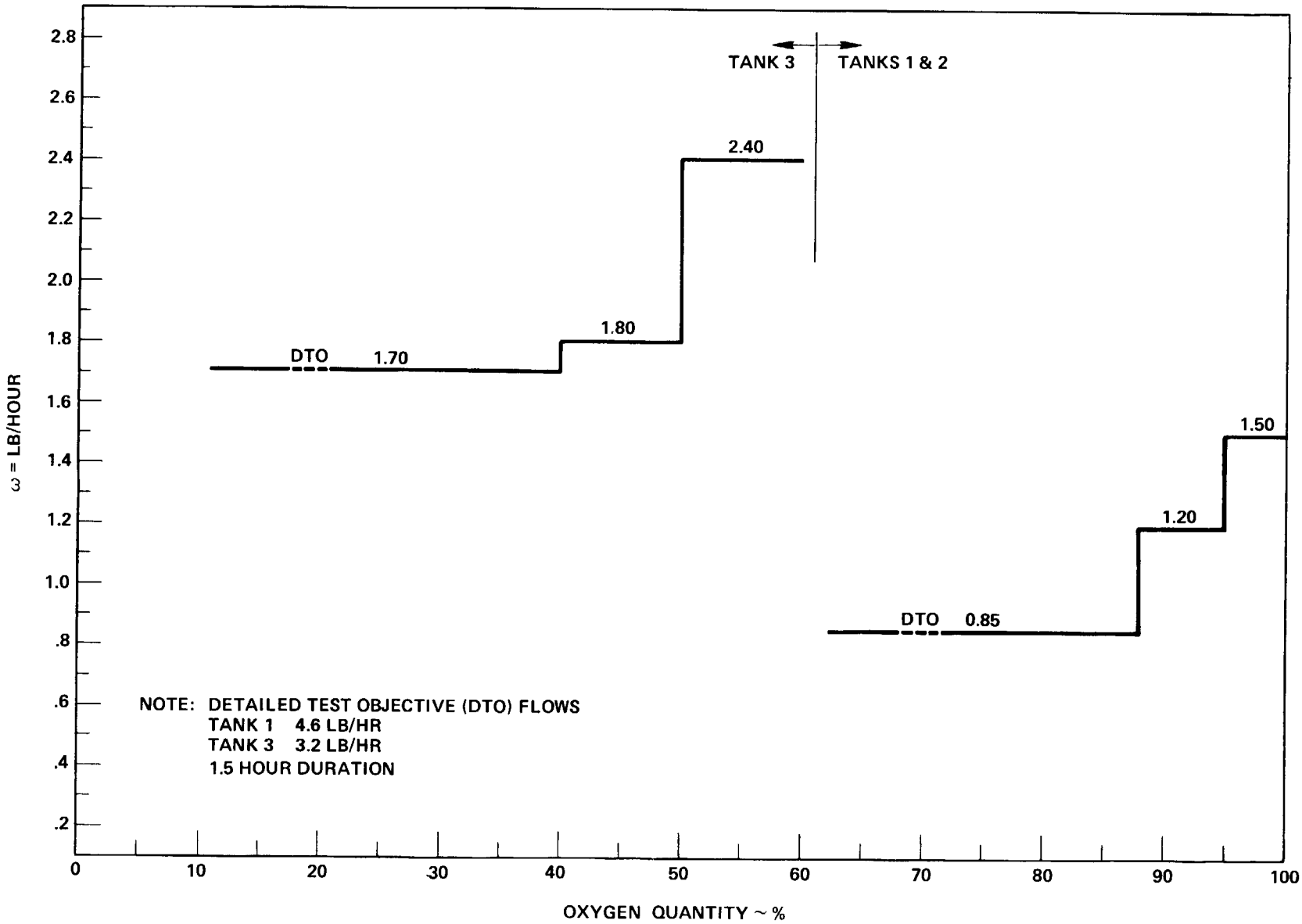

FIGURE 4 - APOLLO 14 AVERAGE O_2 FLOW RATES DURING HEATING OPERATION

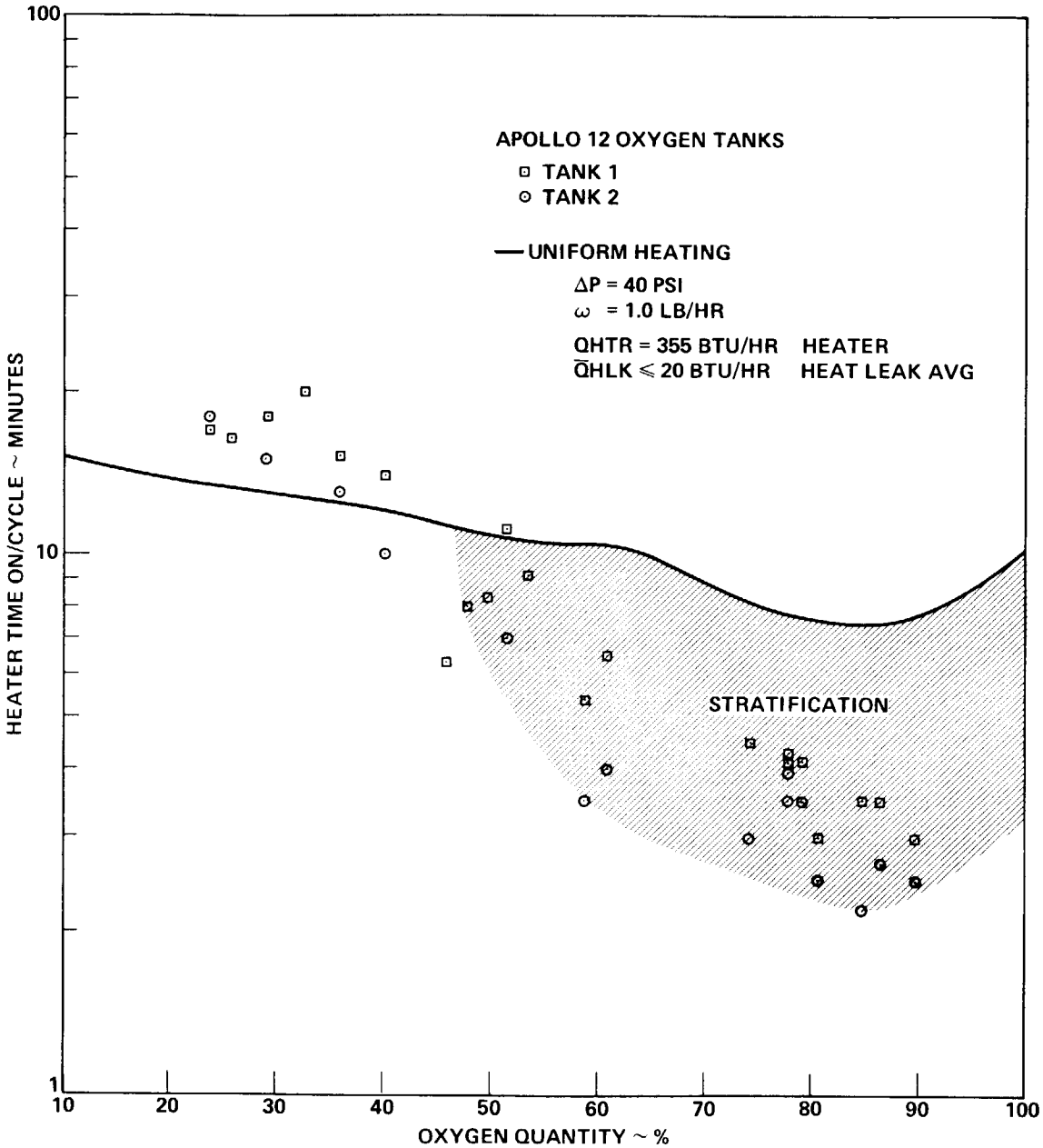

FIGURE 5 - APOLLO 12 PRESSURIZATION TIMES DEPICTING EFFECT OF STRATIFICATION

The average tank flow rates for use in this equation are slightly less than those given in Figure 4 because tank outflow is required to pressurize the remainder of the tank system during each heater operation. Taking this into account, Equation (4) is plotted in Figure 6 with data from Apollo 14. The flight data represent individual pressure cycles. Data lying above the curves reflect a decline of stratification, and below the curves a buildup of stratification. The existence of the former demonstrate that stratification is limited not only by discrete pressure decays but also by more gradual and subtle changes in the state of fluid motion.

II. TWO-FLUID MODEL

A. Physical Description

From the foregoing, it is clear that stratification affects the pressure behavior of the Apollo oxygen tanks. The intent of this investigation has been to evaluate the extent of fluid segregation occurring. That is, to determine how much fluid interacts with the heater during each heater cycle.

While the heater is on, a temperature profile develops in the surrounding fluid. Following heater deactivation, the heat gradually disperses via conduction and convection. The observed buildup of larger pressure decay potentials with time indicates that the energy is not completely dispersed by the time of the next heater cycle. Thus, there is a spectrum of heater temperatures encountered along a radial profile from the heater. It is assumed here that the total amount of fluid composing the heated layers is small. In this case it is of interest to determine the mean properties of the heated volume, as deduced from pressure data. This is the basic premise of the two-fluid model.

The principal aspects of the model are schematically depicted in Figure 7. The fluid volume is assumed to be divided into two parts. The volume near the heater is designated the stratified volume, and the remaining volume is called the bulk volume. While the heater is on, thermal energy passes from the heater to the stratified volume at a rate Q_{HTR}. A portion of this energy may be passed on to the bulk phase, at a rate Q_{SB}. The bulk phase also receives heat through the tank walls at a rate Q_{HLK}. There is assumed to be no mass exchange between the stratified and bulk volumes during this process, and the flow out of the tank is assumed to emanate from the bulk phase alone.

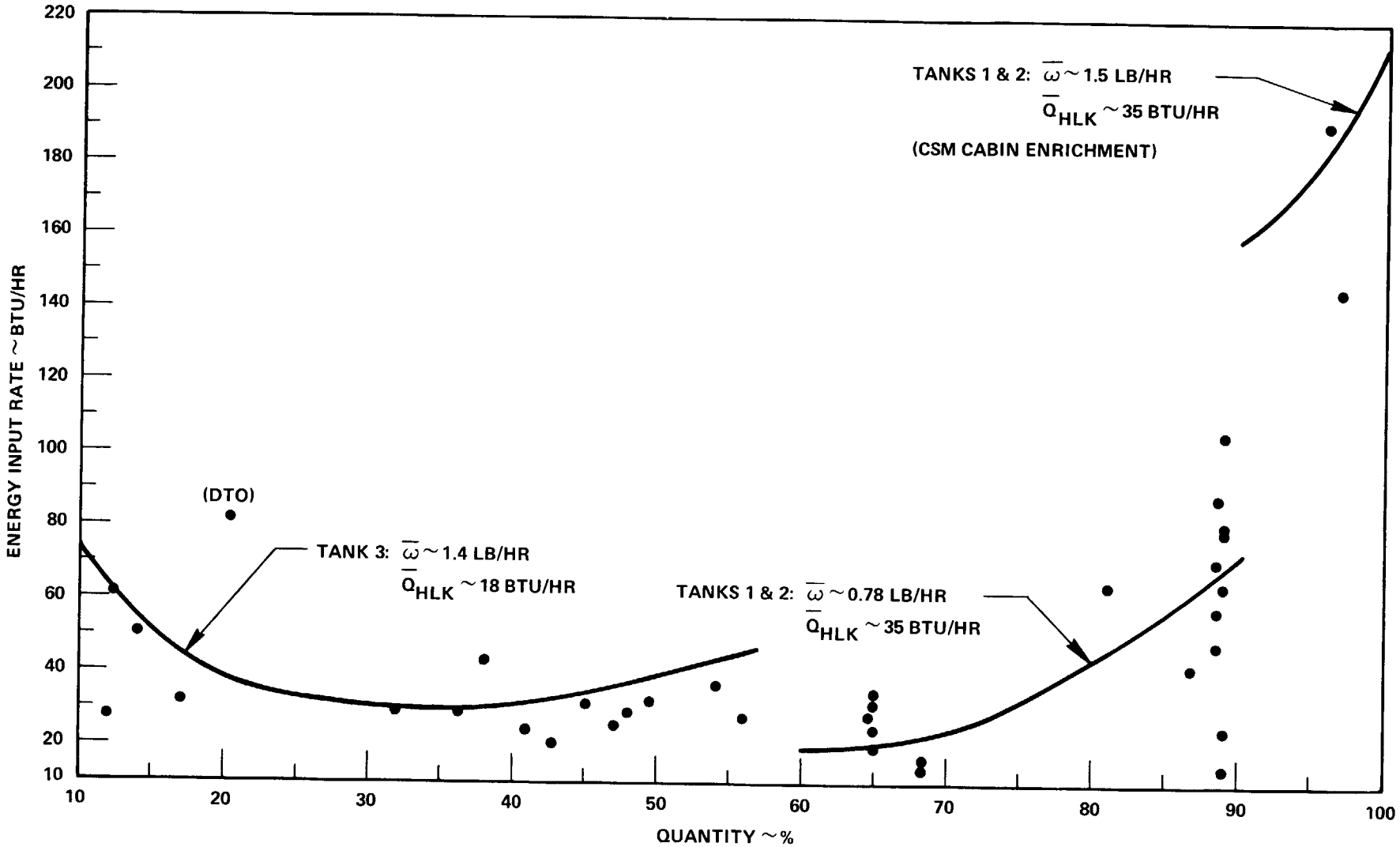

FIGURE 6 - ENERGY INPUT RATE ON APOLLO 14 AS FUNCTION OF QUANTITY AND FLOW RATE

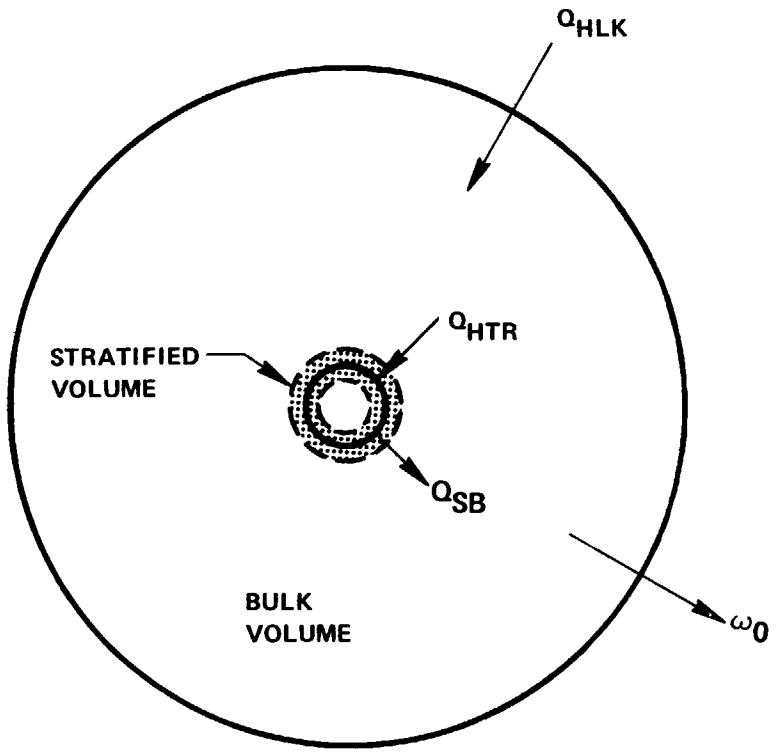

FIGURE 7 - SCHEMATIC OF TWO FLUID MODEL

Since the stratified volume retains the majority of the energy and possesses much smaller mass, its temperature rise is much greater. As the pressure is uniform throughout the tank, the higher temperature of the stratified volume is reflected in a volume expansion. The expanding stratified volume mechanically compresses the bulk fluid.

B. Governing Equations

Each phase is assumed to be homogeneous. Therefore, their pressure histories can be described by Equation (1); for the bulk

$$\dot{p} = \frac{\phi_B}{V_B} \left(Q_B - \rho_B \theta_B \dot{V}_B - \theta_B \omega_0\right) \tag{5}$$

and for the stratified volume

$$\dot{p} = \frac{\phi_S}{V_S} \left(Q_S - \rho_S \theta_S \dot{V}_S\right) \tag{6}$$

where the variables are as previously defined, with the subscripts B and S referring to the bulk and stratified phases, respectively. ω_0 is the rate of mass flow out of the tank. Since uniform pressure is maintained, $\dot{p}$ is the same for both phases.

Equations (5) and (6) can be solved directly for the rate of tank pressure change as a function of energy flux and the amount of stratification. This is done in Appendix C. A more revealing form can be generated, however, by incorporating two simplifying assumptions. The first is that the stratified volume is very small compared to the total volume, V_T, i.e., $V_S/V_T \approx 0$. The second is related to the amount of heat entering the bulk phase. From Figure 7 we see that Q_B comes from two sources, Q_{HLK} and Q_{SB}. It will be assumed that Q_B exactly offsets the effect of tank outflow; that is

$$Q_B = Q_{HLK} + Q_{SB} = \theta_B \omega_0 \tag{7}$$

Solution of Equations (5) and (6) now yields

$$\dot{p} = \frac{\rho_B \theta_B}{\rho_S \theta_S} \frac{C\phi_B}{V_T} Q_T \tag{8}$$

and

$$\dot{V}_S = \frac{Q_T}{\rho_S \theta_S} \tag{9}$$

where Q_T is the total rate of energy transfer into the fluid

$$Q_T \equiv Q_S + Q_B - \Theta_B \omega_0 \tag{10}$$

and C is related to the effect of tank volume change on the pressure change rate. The parameter C is discussed in Appendix B; its variation for the oxygen tank is given in Figure 8.

Equation (8) furnishes insight into the nature of the stratification process. From Appendix B (Equation B18) we find that the pressurization rate for uniform heating, $\dot{p}_U$, is

$$\dot{p}_U = \frac{C\phi_B}{V_T} Q_T \tag{11}$$

From Equation (8) then the ratio of the stratified-to-uniform pressure rise rate, $\dot{p}_S/\dot{p}_U$, is

$$\frac{\dot{p}_S}{\dot{p}_U} = \frac{\rho_B \theta_B}{\rho_S \theta_S} \tag{12}$$

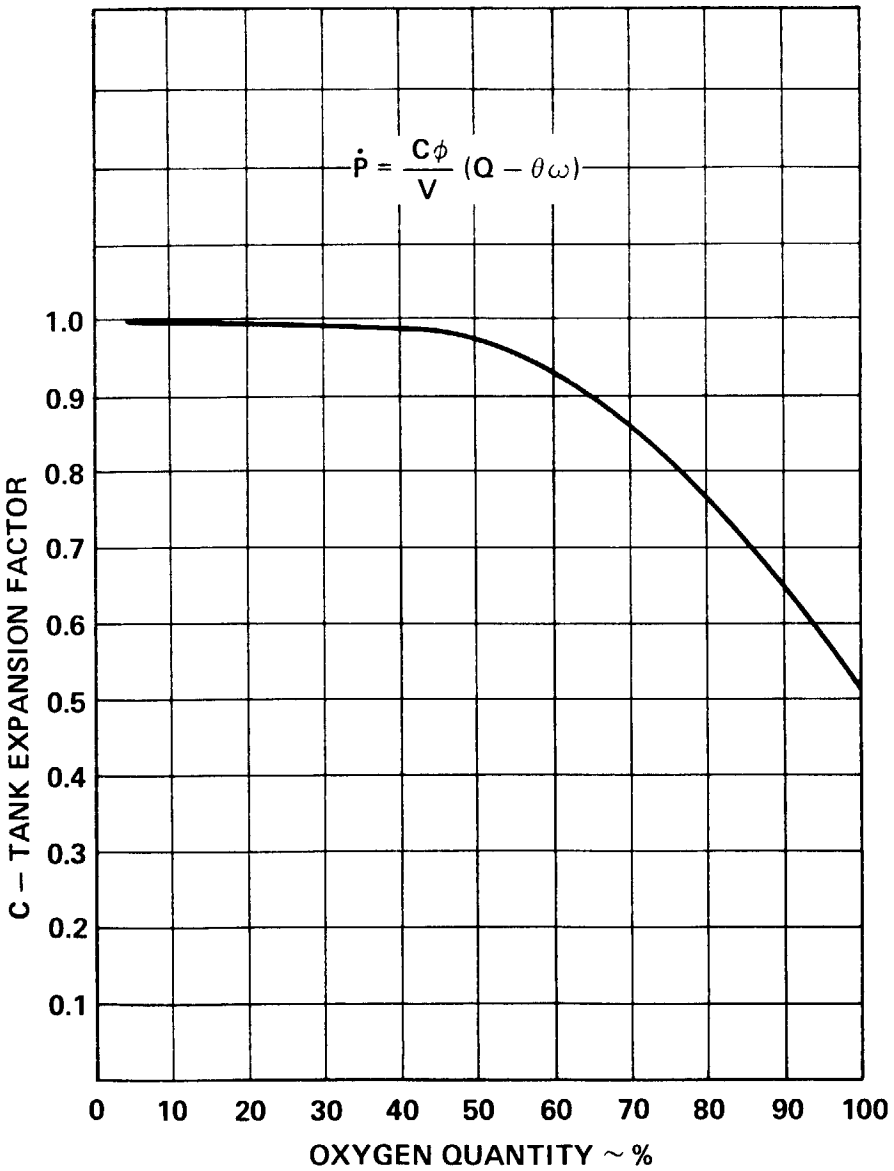

FIGURE 8 - OXYGEN TANK ELASTICITY EFFECT

Figure 9 shows the variation of $\rho\theta$ with density for oxygen. During the stratifying process we work down along the $\rho\theta$ curve, i.e., the density of the stratified volume decreases. For example, if the initial density is 60 lb/ft^3 and stratification has proceeded to the point where the stratified volume has doubled, then

$$\frac{(\rho\theta)_{60}}{(\rho\theta)_{30}} = \frac{6700}{1000} = 6.7 \quad .$$

That is, the pressure rise rate at that point is 6.7 times what it would be in the absence of stratification.

Equations (8) and (9) can be integrated to yield the time variation of the pressure and stratified volume. The resulting expression for pressure is:

$$p - p^I = K_B(V_S - V_S{}^I) \tag{13}$$

where p^I and $V_S{}^I$ are the initial values for pressure and stratified volume, and K_B is a constant of the bulk phase, defined

$$K_B \equiv \rho_B \theta_B \frac{C\phi_B}{V_T} \tag{14}$$

The corresponding stratified volume variation with time is, in terms of stratified density:

$$F(\rho_S) = F(\rho_B) - \frac{Q_T}{m_S}(t - t^I) \tag{15}$$

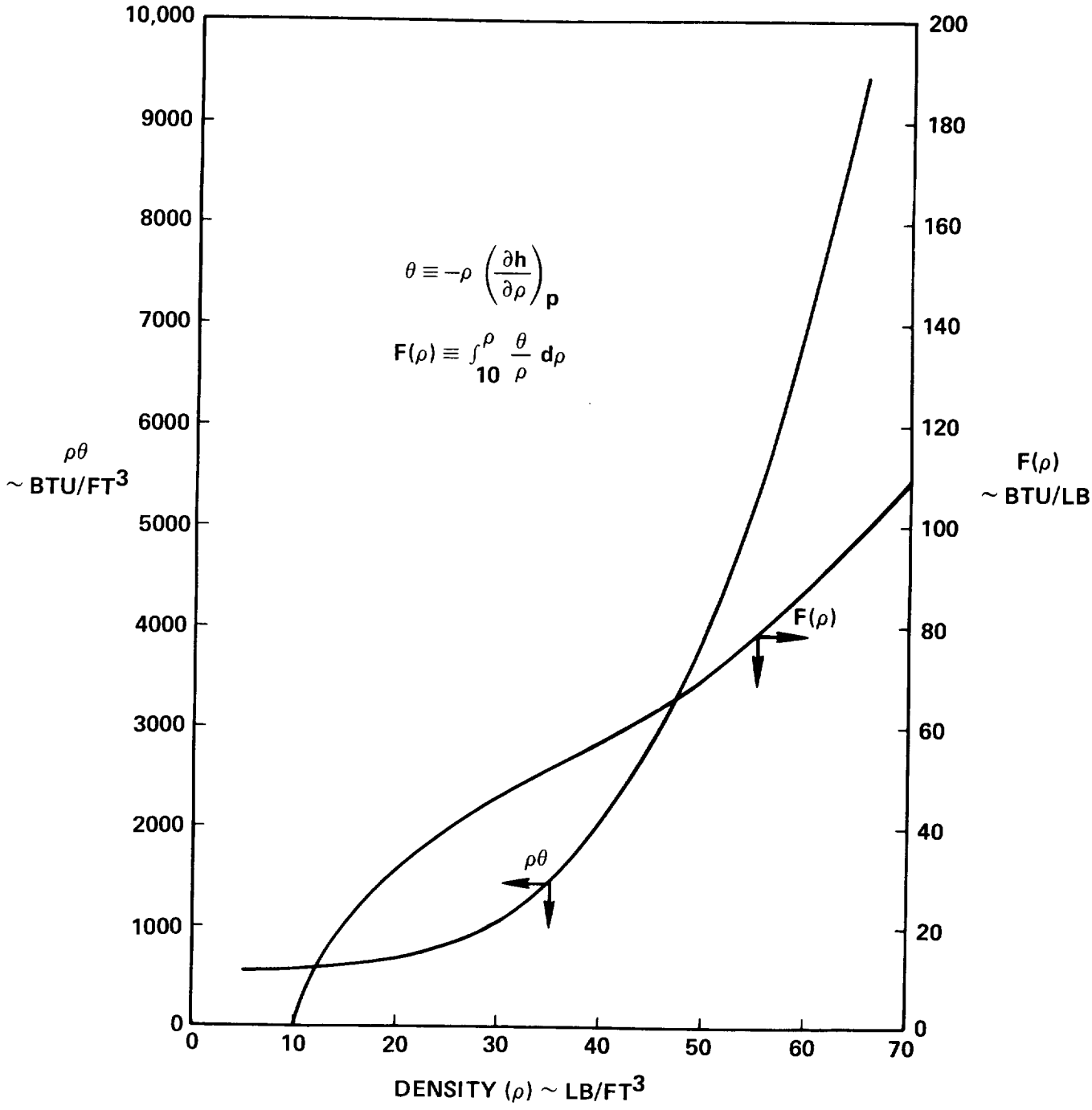

FIGURE 9 - TWO FLUID PARAMETERS

where m_S is the fluid mass in the stratified volume, t^I the initial time, and $F(\rho)$ a state variable, defined

$$F(\rho) \equiv \int_{\rho_R}^{\rho} \frac{\Theta}{\rho} \, d\rho \tag{16}$$

where ρ_R is an appropriate reference density. The variation of $F(\rho)$ with density for a reference density of 10 lb/ft^3 is shown in Figure 9.

Using Equations (13) and (15) the tank's pressure variation with time and energy input can be determined as a function of initial stratified volume and the bulk fluid properties.

III. RESULTS

Two comparisons of the predictions of Equations (13) and (15) with Apollo 14 flight data are shown in Figures 10 and 11, for 82% and 87% tank quantities, respectively. Both tank pressure and heater temperature sensor data are considered. The comparable results for uniform pressurization are also indicated. The stratified volume size was determined by matching the model to the flight data at the highest pressure attained during the heater cycle.

Since the pressure data were fit at the beginning and end of the heater cycle, it is the form of the predicted pressure variation rather than the numerical agreement that is of interest. The prediction undershoots the data at all points intermediate to the final pressure. This can be attributed to the simplification of assuming constant bubble size. That is, if we were to determine the bubble size necessary to match each data point we could specify a steadily growing bubble. This type of bubble growth seems reasonable.

Since the pressure data was used to size the bubble, it is of interest to examine the closeness of the numerical fit to the temperature data. Two aspects of the flight data for heater temperature are pertinent. First, it is known that the temperature sensor is not located at the hottest spot on the heater; the difference between the two temperatures is estimated by Manned Spacecraft Center analysis to range from 9 to 50° F during the heater cycle. Secondly, the temperature sensor is partially insulated from the heater by its housing and so its temperature lags that of the heater when the heater temperature changes. The lag is estimated to be up to 50° F.

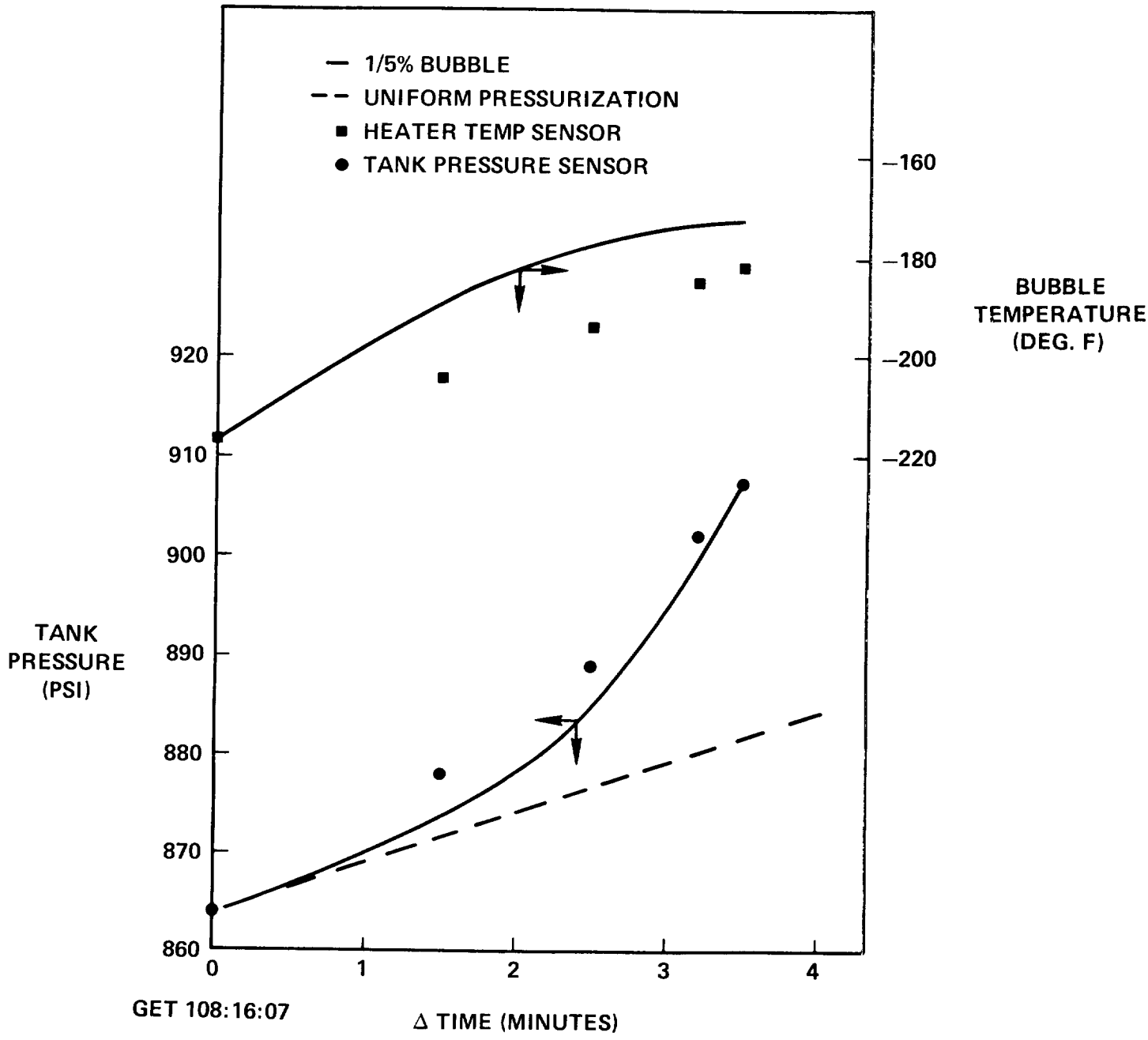

FIGURE 10 - APOLLO 14 HEATER CYCLE: TANK 1 ~ 82%

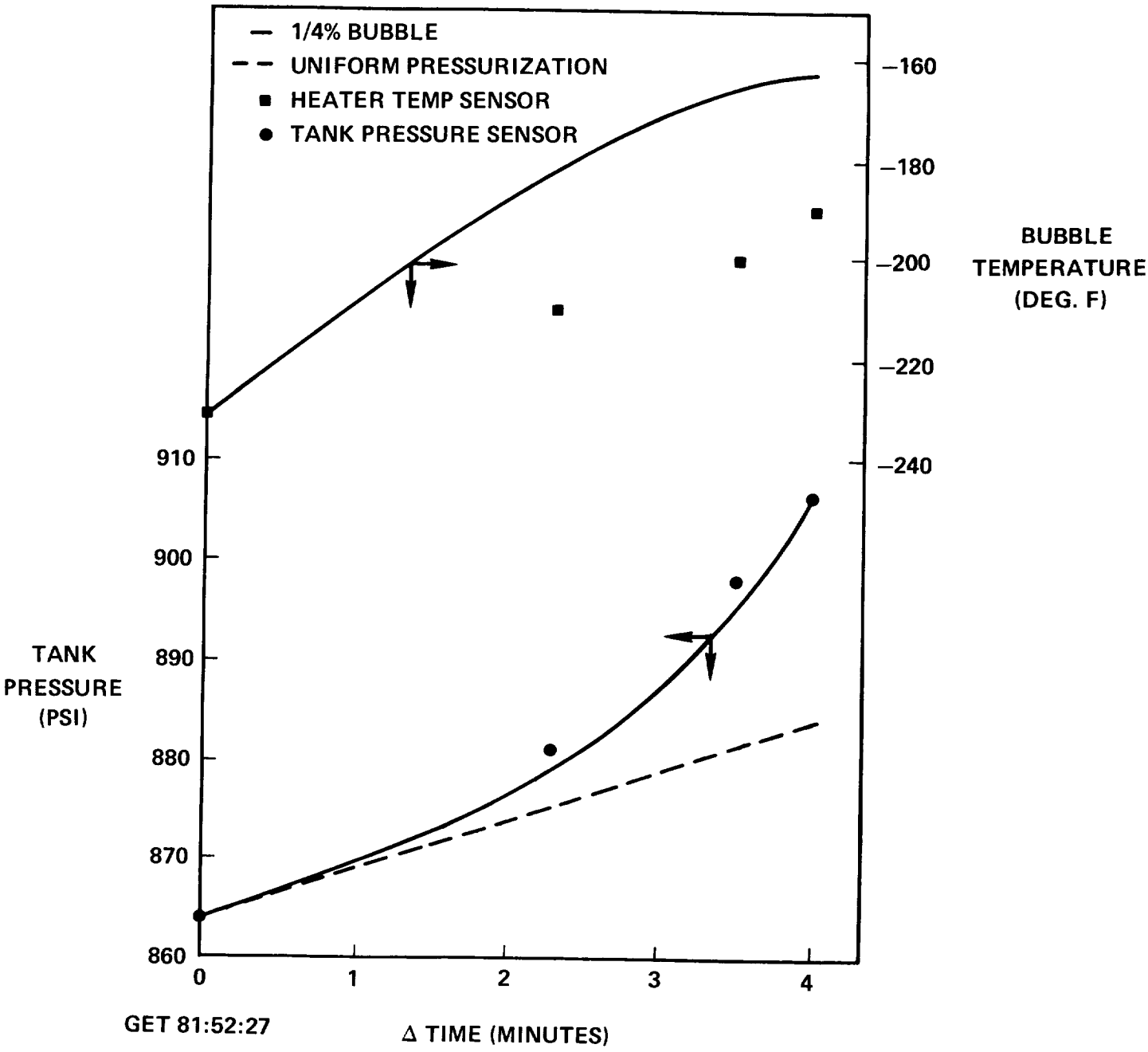

FIGURE 11 - APOLLO 14 HEATER CYCLE: TANK 1 ~ 87%

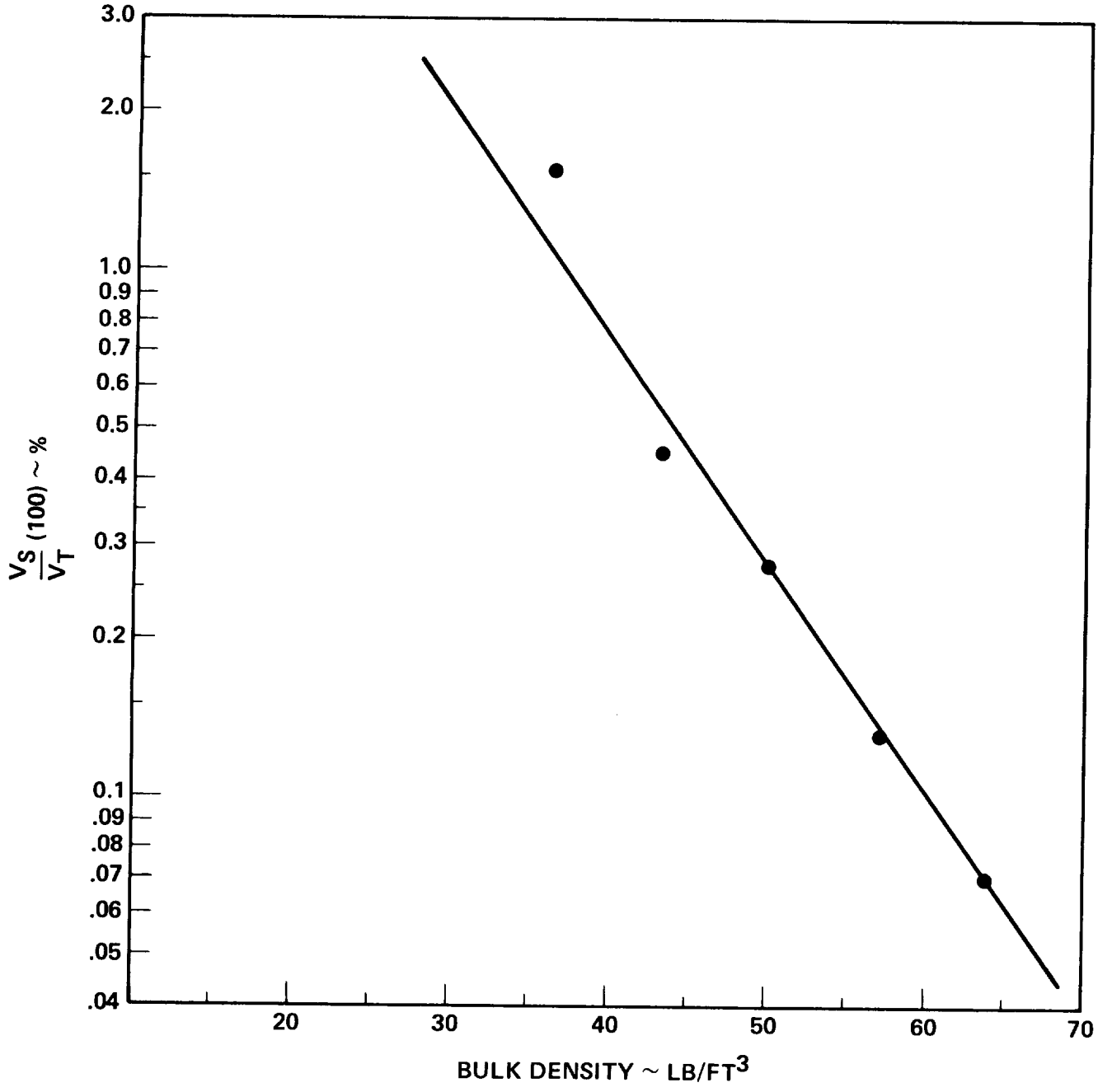

FIGURE 12 - BUBBLE SIZE VARIATION WITH BULK DENSITY

ACKNOWLEDGEMENTS

Appreciation is expressed to Myra Drickman for her expeditious work in programming the equations for the oxygen thermophysical properties; to Al Haron and Sol Fineblum for their computational and analytical assistance; and to Bob Sperry for many helpful suggestions regarding the conceptual aspects of this work.

J. A. Saxton

2031-JAS-jf

Attachments
Nomenclature
References
Appendices A, B, C and D

NOMENCLATURE

VARIABLES

C	tank expansion factor defined by Equation (B17)
C_p	heater specific heat
E	Young's modulus
$F(\rho)$	fluid state variable defined by Equation (16)
h	fluid enthalpy per unit mass
K_B	bulk phase constant defined by Equation (14)
ℓ	tank wall thickness
m	fluid mass
M	heater mass
p	fluid pressure
q	energy flux per unit mass
Q	energy flux
ΔQ	incremental energy flux
r	tank radius
S	tank circumference
t	time
u	fluid internal energy per unit mass
V	volume
y	two fluid parameter defined by Equation (C16)
δ	difference between stratified and uniform cooling in Figure 2
Δ	difference between stratified and uniform heating in Figure 2
ϕ	fluid state variable defined by Equation (2)

θ	fluid state variable defined by Equation (3)
σ	Poisson's ratio
τ	time increment
ω	fluid flowrate

SUBSCRIPTS

B	bulk
ELEC	electrical
HLK	heat leak
HTR	heater
O	out from tank
S	stratified
SB	stratified-to-bulk
STOR	stored
T	total
U	uniform
2,3	tank 2, tank 3

SUPERSCRIPTS

$\cdot$	time derivative
$-$	mean value
I	initial value

REFERENCES

1. MSC Cryogenics Symposium, NASA MSC-04312, May 20-21, 1971.

2. "Absorption Coefficients", NASA-Langley Research Center, Contract No. L-62,510.

3. Haron, A. S., "Transient Analysis fo Heat Transfer in a Simplified Model of the Apollo Oxygen Tank", Bellcomm Memorandum for File B70 12076, December 30, 1970.

4. Forester, C. K., "Pressurized Expulsion of Nonisothermal Single-Phase Cryogen", MSC Cryogenics Symposium, NASA MSC-04312, May 20-21, 1971.

5. Heinmiller, P. J., "A Numerical Solution of the Navier-Stokes Equations for Supercritical Fluid Thermodynamic Analysis", MSC Cryogenics Symposium, NASA MSC-04312, May 20-21, 1971.

6. Suttles, J. T. and Smith, G. L., "Stratification Calculations in a Heated Cryogenic Oxygen Storage Tank at Zero Gravity", MSC Cryogenics Symposium, NASA MSC-04312, May 20-21, 1971.

7. Drickman, M. V., "Calculation of Theta and Phi for Cryogenic Oxygen", Bellcomm Memorandum for File B70 11035, November 16, 1970.

APPENDIX A

APOLLO CRYOGENIC OXYGEN TANKS

Tank Configuration

The principal aspects of the Apollo cryogenic oxygen tank configuration are depicted in Figure 13. There are three tanks* -- two in Bay IV and the third in Bay I of the Service Module. Figure 14 illustrates the Apollo 14 tank interconnections and control devices for providing uniform distribution of oxygen to the environmental control system and the fuel cells.

The 4.76 ft^3 capacity tanks are of dewar design with multilayer insulation filling the annular region. The quantity gauge along the tank centerline is composed of two concentric cylinders employed as capacitors to determine the fluid's dielectric constant, hence furnishing a measure of fluid density. The 1.7 inch O.D. gauge also serves as a standpipe for fluid transfer to and from the tank.

The 1.5 inch O.D. heater, whose centerline is offset 2.18 inches from that of the quantity gauge, furnishes the energy needed to maintain tank pressure while mass removal occurs during flight. Wrapped along the outside of the heater are three separate heater elements, each providing roughly 125 Btu/hr power. There are holes in the heater to enable fluid adjustment during the heater cycles. The heater can be automatically controlled by pressure switches located external to the tank (see Figure 14) or manually controlled by the astronauts, with one- two- or three-heater element operation possible in each case. There are two temperature sensors within the tank, one near the top of the heater and the other at the top of the quantity gauge. The heater temperature sensor is near the hottest spot on the heater; if necessary, the heater is manually controlled so that the sensor output does not exceed 350° F. This temperature red-line protects against either ignition of the Teflon in the quantity gauge or structural weakening of the tank wall.

---

*Only the two Bay IV oxygen tanks were present on flights prior to Apollo 14.

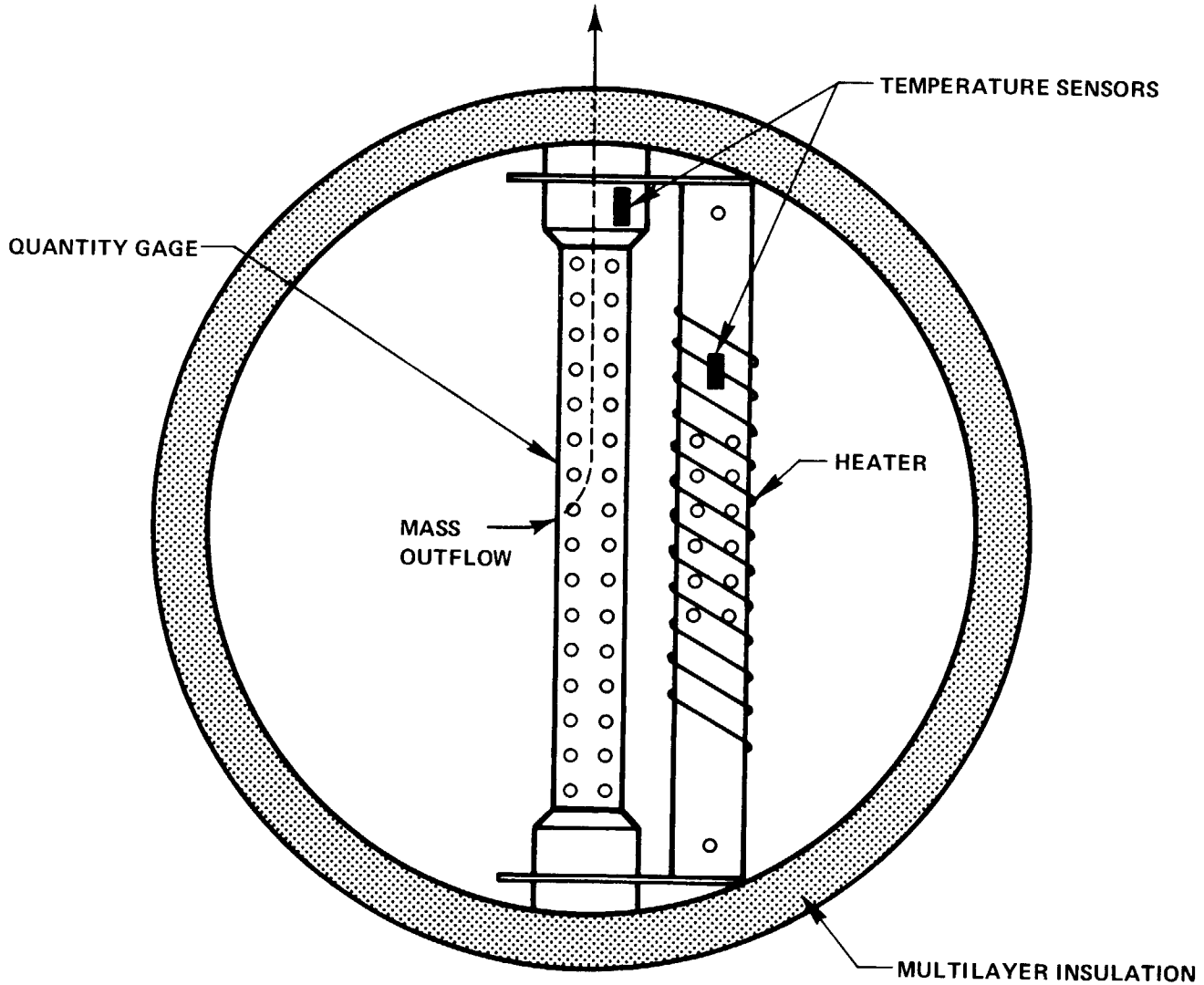

FIGURE 13 - APOLLO CRYOGENIC OXYGEN TANK SCHEMATIC

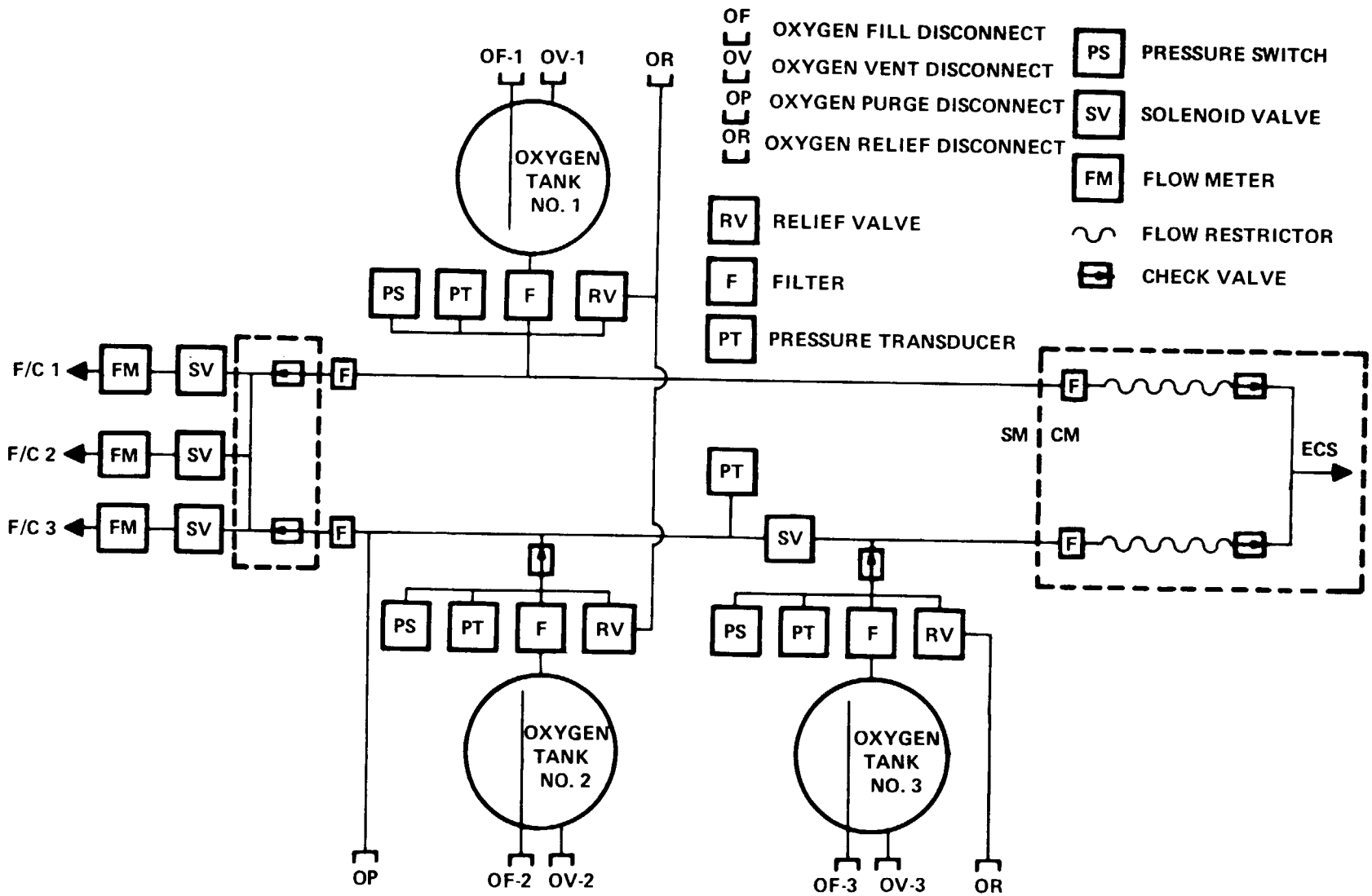

FIGURE 14 - CRYOGENIC OXYGEN SYSTEM

Tank Operation

The tanks are initially loaded with 330 lb. liquid oxygen at atmospheric pressure. Heat is then added to achieve the tank's 900 psia operating pressure. During the prelaunch period heat leak through the vessel walls causes the tank pressure to rise gradually to the upper pressure switch setting at which point venting occurs. Once power is switched to the fuel cells, sufficient demand for oxygen exists that venting no longer occurs. As oxygen is withdrawn during flight, the heaters are cycled under the control of the pressure switches to maintain pressure at 900 ± 35 psia (nominal).

The pressure-quantity history of the tank during the mission is indicated by Figure 15. On the abscissa, 100% quantity corresponds to 330 lb. oxygen at 69.5 lb/ft^3 density and 0% quantity corresponds to 6.6 lb. oxygen (residual). The heater maintains tank pressure within the indicated operating band. Thus, the fluid is kept in a super-critical state throughout, passing above the two phase region. This is done for reasons of accuracy in quantity determination, smoothness of energy addition, and uniformity of tank outflow. The lower operational limit, based on the demands from other spacecraft systems, is 150 psia required for fuel cell feed.

Apollo 14 Tank Usage

It was desired on Apollo 14 to observe tank operation at both high and low densities. Since normal usage would not lower the quantity in any tank down to the low quantity regime of interest, 20% and below, Tank 3 was offloaded to 60% prior to lift off. This tank was then utilized as the primary source of oxygen during the translunar coast (TLC) phase in order to preferrentially reduce its quantity level still further. The usage profiles and heater operational modes are shown in Figure 16.

A Detailed Test Objective (DTO) was conducted at GET 168:10 during the Transearth Coast (TEC). The vehicle was maintained in attitude hold during the test. The DTO was designed to simulate the high flow rates of the EVA's planned for Apollo 15 and beyond. The flight oxygen usage profile was tailored to produce 70% and 20% quantities in Tanks 1 and 3, respectively, at the time of the DTO. Thus, the ability to support high flow at both high and low density was tested. The flowrates were 4.6 and 3.2 lb/hr from Tanks 1 and 3, respectively. The excess flow was routed through the cabin and out a vent valve in the hatch. During the test the urine dump valve was opened, increasing the

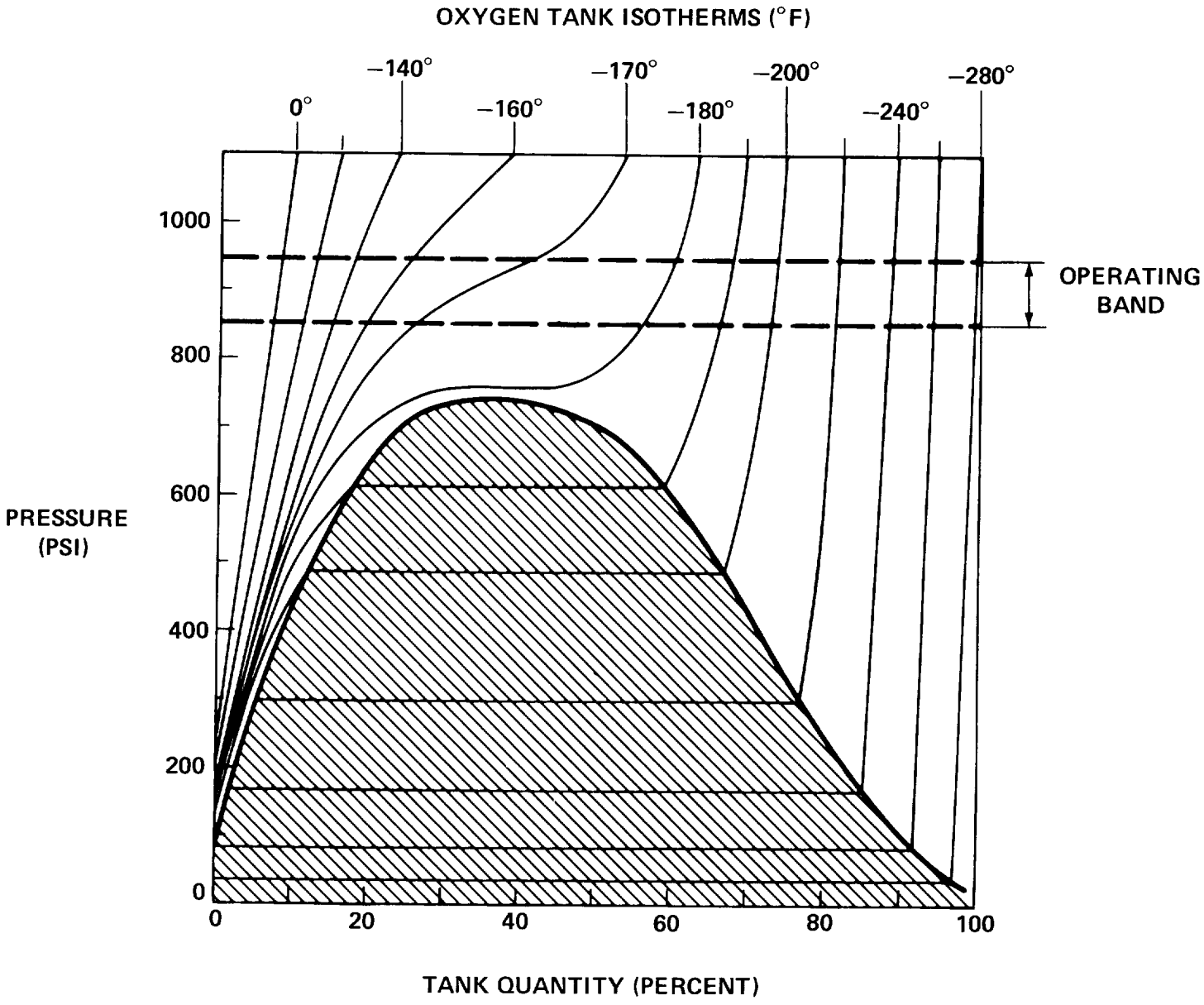

FIGURE 15 - OXYGEN SUPPLY PRESSURE VERSUS TANK QUANTITY

over-board flow beyond acceptable limits. The high flow lowered the cabin pressure, and the test was terminated after 1 hr; a 2.5 hour test had been planned. Post flight analysis indicated that sufficient data was obtained to substantiate system performance at high flows.*

There were two aspects of system performance that affected the pressure rise rates observed. First, the check valve on Tank 2 leaked in such a manner that when Tank 3 alone was supplying the system, equal pressure was maintained in Tanks 2 and 3 by flow from Tank 3 into Tank 2. This extended the heater cycles for Tank 3 by increasing the tank's mass outflow during the pressurization period, and furnishing a supplementary flow during the depressurization period. Secondly, the Tank 3 heater temperatures, as indicated by the heater temperature sensor, were increasing rapidly as lower quantities were encountered. In order to maintain the temperature below a redline of 350° F, the heater in Tank 3 was switched to 2/3 power below 41%, with the exception of two inadvertant full power cycles following the DTO. As anticipated, the lower power led to longer heater cycles for Tank 3.

---

*System performance on Apollo 15 confirmed the analysis.

APPENDIX B

TANK PRESSURE VARIATION WITH ENERGY AND MASS FLUX

The thermodynamic response of a unit mass of oxygen to energy and density changes is given by the first law of thermodynamics:

$$du = dq + \frac{p}{\rho^2}\, d\rho \tag{B1}$$

where u and q are the internal energy and energy flux per unit mass and p and ρ are the pressure and density. The internal energy dependence upon pressure and density can be expressed:

$$du = \left(\frac{\partial u}{\partial p}\right)_\rho dp + \left(\frac{\partial u}{\partial \rho}\right)_p d\rho \tag{B2}$$

Solving Equations (B1) and (B2) for the pressure change by eliminating the internal energy, we get:

$$dp = \frac{dq + \left[\frac{p}{\rho^2} - \left(\frac{\partial u}{\partial \rho}\right)_p\right] d\rho}{\left(\frac{\partial u}{\partial p}\right)_\rho} \tag{B3}$$

We differentiate both sides with respect to time and introduce the following relations:

$$\left(\frac{\partial h}{\partial \rho}\right)_p = \left(\frac{\partial u}{\partial \rho}\right)_p - \frac{p}{\rho^2} \tag{B4}$$

$$\dot{\rho} = \frac{1}{V}\left(\dot{m} - \rho \dot{V}\right) \tag{B5}$$

and

$$\omega \equiv -\dot{m} \tag{B6}$$

where the dot superscript indicates a time derivative. The result is

$$\dot{p} = \frac{Q + \rho\left(\frac{\partial h}{\partial \rho}\right)_p (\omega + \rho\dot{V})}{V\rho\left(\frac{\partial u}{\partial p}\right)_\rho} \tag{B7}$$

where Q is the total energy flux into the system.

We define the variables

$$\theta \equiv -\rho\left(\frac{\partial h}{\partial \rho}\right)_p \tag{B8}$$

$$\phi \equiv \frac{1}{\rho}\left(\frac{\partial p}{\partial u}\right)_\rho \tag{B9}$$

and substitute them into Equation (B7) to obtain:

$$\dot{p} = \frac{\phi}{V}(Q - \rho\theta\dot{V} - \theta\omega) \tag{B10}$$

If the volume change $\dot{V}$ is a result solely of tank stretch with increasing pressure, Equation (B10) can be put into a more specific form. The volume change can be expressed:

$$\dot{V} = \dot{p}\left(\frac{dV}{dp}\right) \tag{B11}$$

or in terms of radial change for a spherical volume

$$\dot{V} = \dot{p} \cdot \frac{3V}{r} \cdot \left|\frac{dr}{dp}\right| \tag{B12}$$

The change of radius dr with pressure is equivalent to

$$\frac{dr}{dp} = \frac{dr}{dS}\frac{dS}{dp} \tag{B13}$$

where S is the circumference. From structural analysis we know that for a sphere

$$\frac{dr}{dS} = \frac{r}{E}(1-\sigma) \tag{B14}$$

and

$$\frac{dS}{dp} = \frac{r}{2\ell} \tag{B15}$$

where E, σ, ℓ are Young's Modulus, Poisson's ratio, and tank wall thickness, respectively. Substituting Equations (B12), (B13), (B14), and (B15) into Equation (B10) and rearranging, we get:

$$\dot{p} = \frac{\frac{\phi}{V}(Q - \omega\theta)}{1 + \frac{3(1-\sigma)r}{2E\ell}\rho\theta\phi} \tag{B16}$$

We now define a parameter C that includes all factors arising from tank volume change

$$C \equiv \left(1 + \frac{3(1-\sigma)r}{2E\ell}\rho\theta\phi\right)^{-1} \tag{B17}$$

so that

$$\dot{p} = \frac{C\phi}{V}(Q - \theta\omega) \qquad \text{(B18)}$$

For Apollo tanks

$r = 12.53$ inches

$\ell = 0.059$ inches

$E = 3 \times 10^7$ psi

$\sigma = 0.29$

Then

$$C = (1 + 7.545 \times 10^{-6}\ \rho\theta\phi)^{-1} \quad . \qquad \text{(B19)}$$

The variation of C with respect to oxygen quantity is shown in Figure 8. We see that at the higher quantities tank volume expansion significantly decreases the rate of pressure rise.

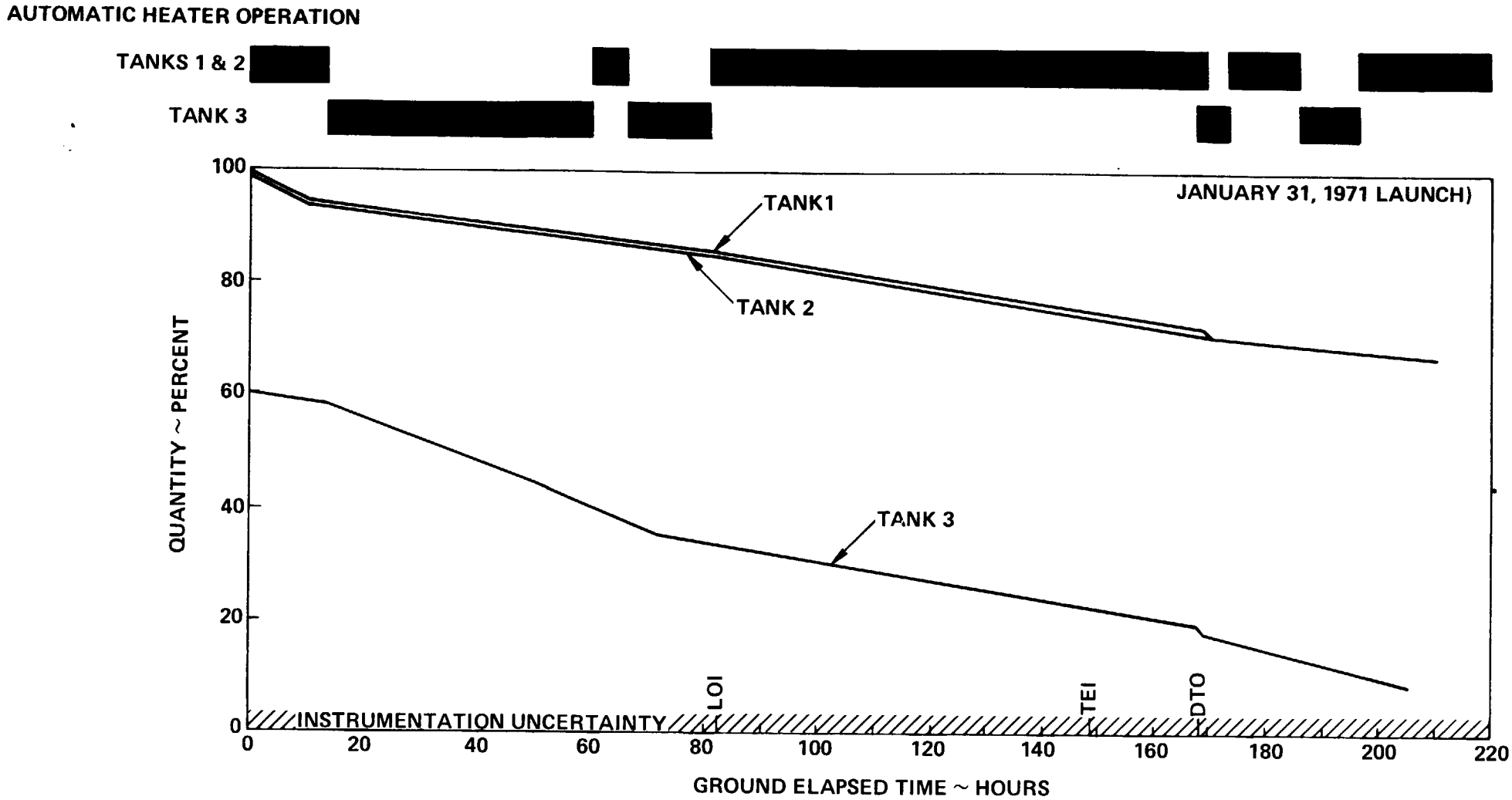

FIGURE 16 - APOLLO 14 OXYGEN USAGE AND HEATER OPERATION PROFILES

APPENDIX C

TWO-FLUID-MODEL EQUATION DERIVATIONS

General Form

In the two fluid model, the total fluid volume is considered divided into two portions as shown in Figure 7. Each portion is taken to be homogeneous. Their pressure variations with energy and mass flux are then given by Equation (B10). The resulting expressions are: for the bulk

$$\dot{p} = \frac{\phi_B}{V_B} \left(Q_B - \rho_B \theta_B \dot{V}_B - \theta_B \omega_0\right) \tag{C1}$$

and for the stratified volume

$$\dot{p} = \frac{\phi_S}{V_S} \left(Q_S - \rho_S \theta_S \dot{V}_S\right) \quad . \tag{C2}$$

The variables are as previously defined and the subscripts denote the bulk fluid B and the stratified volume S. Mass flows out of the tank from the bulk alone at a rate ω_0 and there is no mass interchange between the two volumes. $\dot{p}$ is the same for both volumes as there is uniform pressure throughout the tank.

The stratified volume heating rate Q_S is the energy entering from the heater Q_{HTR} less that leaking to the bulk phase Q_{SB}. The bulk volume heating rate Q_B is the sum of the tank heat leak Q_{HLK} and the leakage from the stratified volume Q_{SB}. The bulk volume can be expressed as the difference between the total volume and the stratified volume

$$V_B = V_T - V_S \tag{C3}$$

and similarly the rate of bulk volume change equals

$$\dot{V}_B = \dot{V}_T - \dot{V}_S \tag{C4}$$

As in Appendix B, the rate of total volume change can be equivalently expressed

$$\dot{V}_T = \dot{p} \frac{dV_T}{dp} \tag{C5}$$

It is convenient to introduce two new parameters:

$$y \equiv \frac{\rho_B \Theta_B}{\rho_S \Theta_S} \tag{C6}$$

$$Q_T \equiv Q_S + Q_B - \Theta_B \omega_0 \tag{C7}$$

y is the ratio of the energy required to produce unit volume change of the bulk phase to that for the stratified phase, and Q_T is the total rate of energy input to the fluid.

Using these parameters we solve for $\dot{p}$ from Equations (C1), (C2), (C3), (C4), and (C5) by eliminating the bulk volume V_B and the volume change rates $\dot{V}_S$, $\dot{V}_B$, and $\dot{V}_T$. The result is

$$\dot{p} = \frac{\phi_S[(y-1)Q_S + Q_T]}{(y - \frac{\phi_S}{\phi_B}) V_S + \frac{\phi_S}{\phi_B} \frac{V_T}{C}} \tag{C8}$$

If instead we solve for $\dot{V}_S$ by eliminating V_B, $\dot{V}_B$, $\dot{V}_T$, and $\dot{p}$, we get

$$\dot{V}_S = \frac{Q_S[V_S(1 - \frac{\phi_S}{\phi_B}) + \frac{V_T}{C}\frac{\phi_S}{\phi_B}] - Q_T V_S}{\rho_S \theta_S[(y-1)V_S + \frac{V_T}{C}]} \qquad (C9)$$

Equations (C8) and (C9) enable a parametric study of the effect of stratification on pressure rise rates. For example, starting from uniform conditions throughout the tank, an initial bubble volume is assumed and values set for the split of energy between phases, Q_S and Q_T. Equations (C3), (C4), (C5), (C8), and (C9) are then solved for the pressure change and the volume change of each phase during the first time step. The new values for the parameters y, ϕ_S, ϕ_B are then calculated and the process repeated for succeeding time steps. The proper initial bubble volume is that leading to the observed pressure rise in the time interval of interest.

Simplified Form

A simplified formulation of the two-fluid model can be generated by introducing two assumptions. The first is that the stratified volume is very small compared to the total volume, so $V_S/V_T \approx 0$. The second is that the amount of heat entering the bulk phase, Q_{HLK} and Q_{SB}, exactly offsets the effect of tank outflow; that is

$$Q_B = Q_{HLK} + Q_{SB} = \theta_B \omega_0 \quad . \qquad (C10)$$

In this case, Equation (C7) becomes

$$Q_T = Q_S = Q_{HTR} + Q_{HLK} - \theta_B \omega_0 \qquad (C11)$$

and Equations (C8) and (C9) are considerably simplified. They become

$$\dot{p} = y \frac{C\phi_B}{V_T} Q_T = \frac{\rho_B \theta_B}{\rho_S \theta_S} \frac{C\phi_B}{V_T} Q_T \tag{C12}$$

and

$$\dot{V}_S = \frac{Q_T}{\rho_S \theta_S} \tag{C13}$$

Equations (C12) and (C13) can be integrated to yield the time variation of the pressure and stratified volume. Equation (C12) can be written

$$\dot{p} = \frac{K_B Q_T}{\rho_S \theta_S} \tag{C14}$$

where

$$K_B \equiv \rho_B \theta_B \frac{C\phi_B}{V_T} \tag{C15}$$

K_B is a constant of the bulk phase, i.e., does not change during the pressure cycle. The integral of Equation (C14) can be expressed

$$p - p^I = \int_0^t \dot{p} dt = \int_{\rho_B}^{\rho_S} \dot{p} \frac{dt}{d\rho} d\rho \tag{C16}$$

where p^I is the initial pressure. Since the mass in the stratified volume, m_S, is constant.

$$\frac{d\rho}{dt} = - \frac{\rho_S^2}{m_S} \dot{V}_S = - \frac{Q_T}{m_S} \frac{\rho_S}{\theta_S} \quad . \tag{C17}$$

Substituting Equations (C14) and (C17) into Equation (C16) we obtain the integral

$$p - p^I = - K_B m_S \int_{\rho_B}^{\rho_S} \frac{d\rho}{\rho^2} = K_B m_S \left(\frac{1}{\rho_S} - \frac{1}{\rho_B}\right) \tag{C18}$$

or

$$p - p^I = K_B (V_S - V_S{}^I) \quad . \tag{C19}$$

The time dependence of the stratified density can be obtained from Equation (C13):

$$\frac{Q_T}{m_S} (t - t^I) = \int_{\rho_S}^{\rho_B} \frac{\theta}{\rho} \, d\rho \tag{C20}$$

where t^I is the time at initial heater activation. We define a new state variable

$$F(\rho) \equiv \int_{\rho_R}^{\rho} \frac{\theta}{\rho} \, d\rho \tag{C21}$$

where ρ_R is a designated reference density. The variation of $F(\rho)$ with density for a reference density of 10 lb/ft^3 is shown in Figure 9. The variation of density with time can now be stated as:

$$F(\rho_S) = F(\rho_B) - \frac{Q_T}{m_S} (t - t^I) \qquad (C22)$$

Using Equations (C19) and (C22) the pressure variation with time can be determined.

APPENDIX D

SAMPLE CALCULATIONS

Energy Storage in the Heater

The heater retains part of the electrical energy dissipated in it, resulting in an increase in heater temperature. Eventually a steady state temperature is attained at which the high heater temperature furnishes sufficient driving force to transfer all the incoming heat to the fluid and tank walls. The heating periods are seldom long enough to reach steady state, however, so generally not all of the electrical energy is available to promote the fluid pressure rise.

The rate of energy storage in the heater is related to its temperature rise rate by

$$Q_{STOR} = M\, C_p\, \dot{\bar{T}} \qquad (D1)$$

where Q_{STOR} is the rate of energy storage in the heater mass M, C_p is the heater specific heat, and $\dot{\bar{T}}$ is the rate of change of the mean heater temperature. We cannot precisely determine $\dot{\bar{T}}$ because we measure the temperature at only one point on the heater and even at that point the temperature sensor lags the true temperature due to thermal resistance between the heater and sensor. The calculated temperature profile along the heater and a comparison with flight data are shown in Figure 17. The heater wiring is more closely wrapped at each end, as depicted in the figure, to produce a more uniform temperature distribution. Since the sensor location near the heater hot spot and the sensor time lag produce counteracting effects, we will assume that the sensor furnishes a reasonable approximation for the mean heater temperature.

Typical temperature profiles are shown in Figure 18. The temperature rise rates for the two cycles are roughly 1040° F/hr. The mass and heat capacity of the Apollo 14 heater were 0.634 lb. and 0.11 Btu/lb/°F, respectively. Therefore, we calculate that the heat stored in the heater is

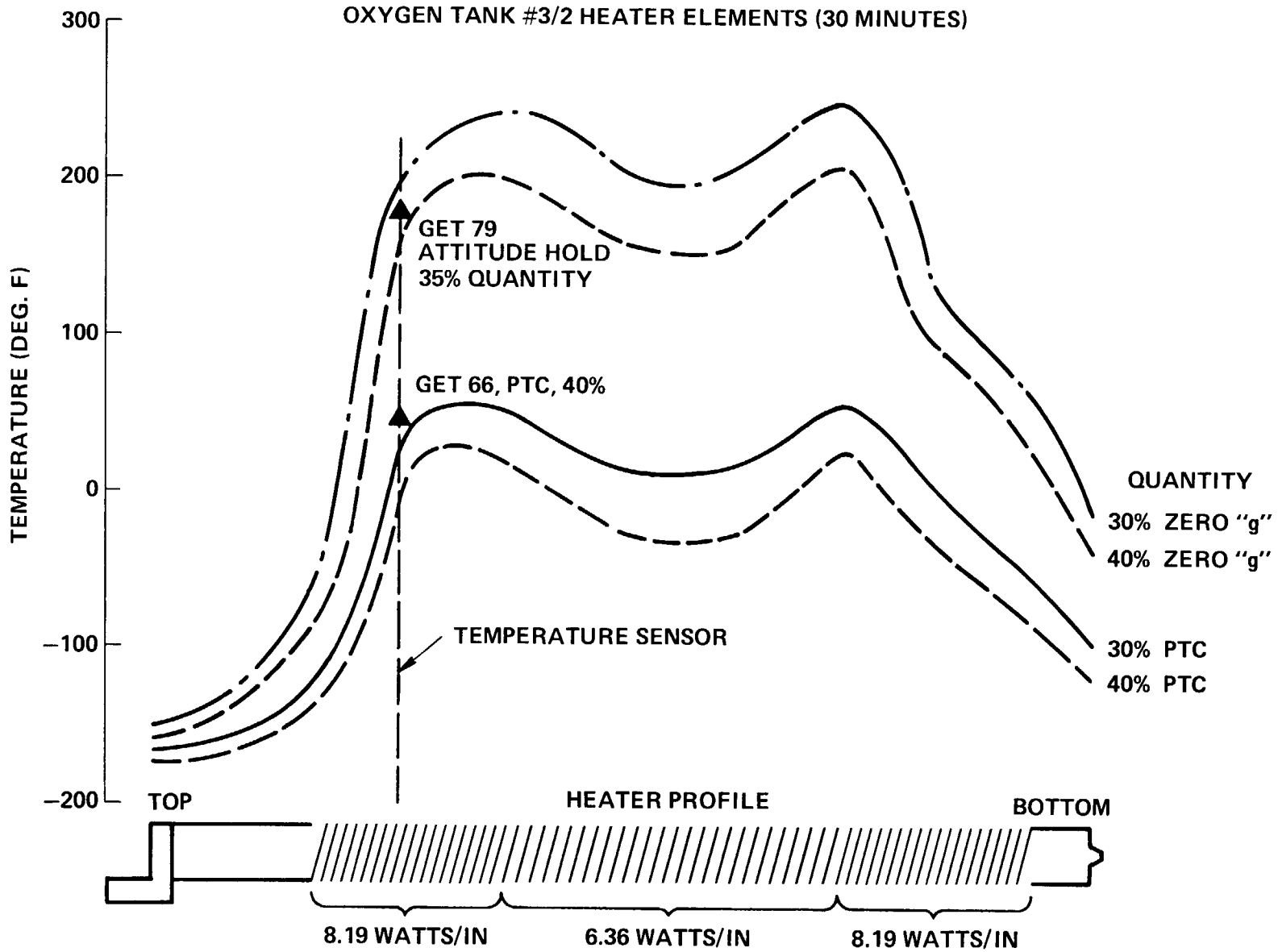

FIGURE 17 - APOLLO 14 HEATER TEMPERATURE PROFILE

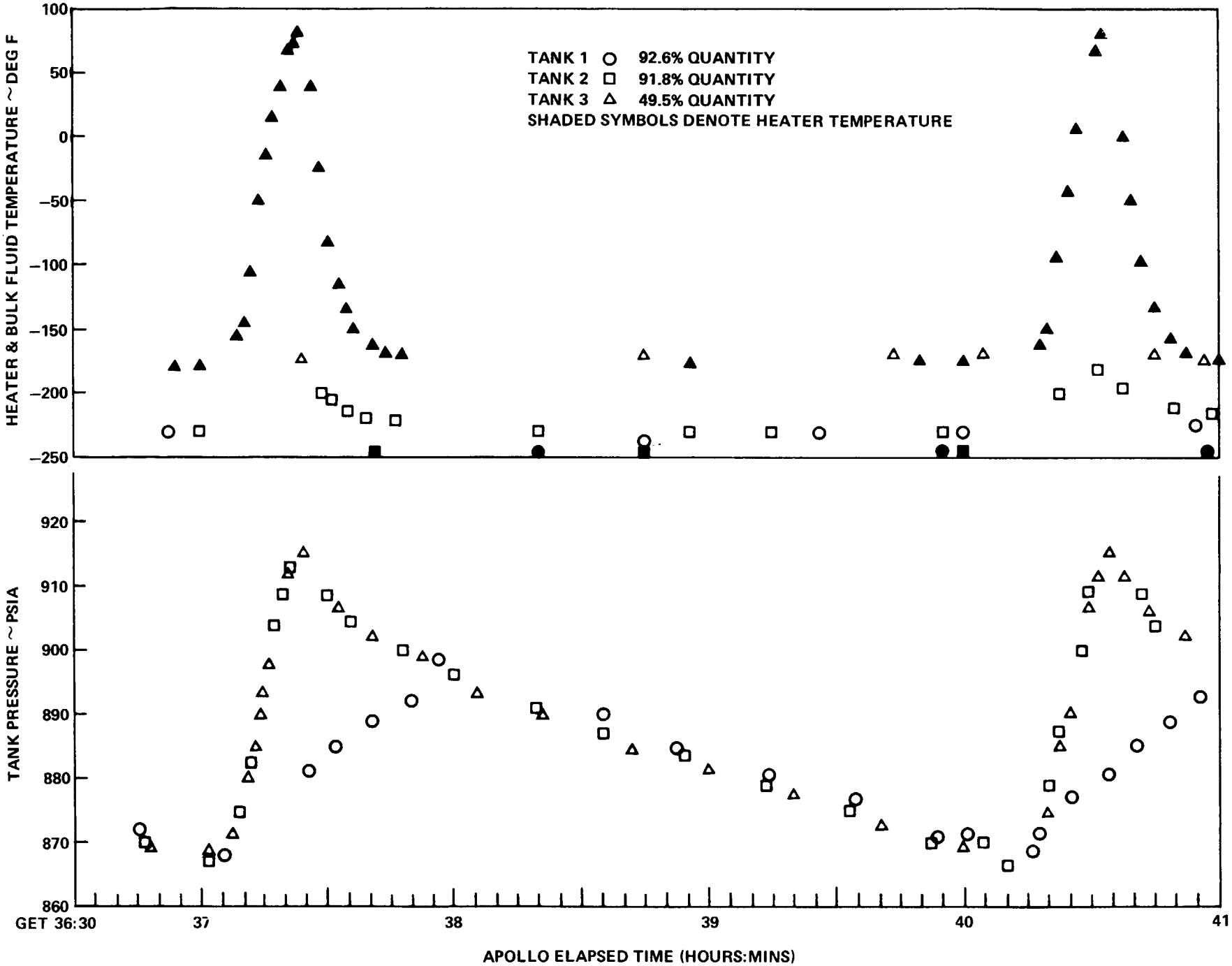

FIGURE 18 - APOLLO 14 PRESSURE AND TEMPERATURE DATA, TANK 3 HEATER ACTIVE

$$Q_{STOR} = (0.634 \text{ lb})(0.11 \frac{\text{Btu}}{\text{lb } °\text{F}})(1000 \frac{°\text{F}}{\text{hr}}) = 70 \frac{\text{Btu}}{\text{hr}}$$

Average Energy Input Rate

This calculation should be done over a period of many heater cycles so that the effect of stratification is averaged out. The principles can be illustrated, however, by considering the pressure cycle shown in Figure 18. The heater on-time is 15 minutes and heater off-time is 174 minutes. Thus,

$$\bar{Q}_{HTR} = \frac{\tau_{ON}}{\tau_{TOTAL}} Q_{ELEC} \qquad \text{(D2)}$$

$$= \frac{15}{189} 375 = 30 \frac{\text{Btu}}{\text{hr}}$$

Over the total cycle there has been no change in pressure, so by Equation (4)

$$Q = \Theta\omega \qquad \text{(D3)}$$

Since Tank 3 contains 49.5% quantity at this time, $\Theta = 38 \frac{\text{Btu}}{\text{lb}}$ (Figure 1). Based on the quantity gauge readings, the flow rate is $1.28 \frac{\text{lb}}{\text{hr}}$. Therefore,

$$Q = (38 \frac{\text{Btu}}{\text{lb}})(1.28 \frac{\text{lb}}{\text{hr}}) = 49 \frac{\text{Btu}}{\text{hr}}$$

Part of this heat is supplied by heat leak. At 49.5% and 1.28 $\frac{lb}{hr}$, Figure 19 indicates a heat leak of 16 $\frac{Btu}{hr}$. Thus, the heat to be supplied by the heater is

$$Q_{HTR} = 49 - 16 = 33 \frac{Btu}{hr} .$$

The close agreement between $\bar{Q}_{HTR}$ and Q_{HTR} is in accord with our findings that thermal stratification does not significantly affect pressure behavior below 50%.

Mass Flow Rate

The flows from the oxygen tanks must supply system requirements, primarily for fuel cell operation and crew respiration. The majority of the flow at any time is supplied by the tanks with active heaters, while the inactive tanks supply low flows due to their heat leak. The quantity gauge readings were used to estimate flow rates during heater operation. It was found that for normal operations on Apollo 14 the active tanks supplied 1.7 lb/hr. Tanks 1 and 2 jointly supply this flow, i.e., 0.85 lb/hr each, while Tank 3 supplies the flow by itself. At the beginning of the mission, Tanks 1 and 2 also support CSM oxygen enrichment and LM pressurization; the flow rates from each tank during these periods are 1.5 and 1.2 lb/hr respectively.

Because of a leaky check valve on Tank 2, its pressure was maintained equal to or greater than that of the intertank plumbing. Consequently, during Tank 3 pressurization cycles sufficient oxygen flowed into Tank 2 to maintain its pressure equal to that of Tank 3, as seen in Figure 18. Thus, during Tank 3 heating periods its outflow rate was increased by an amount sufficient to replace the oxygen that entered Tank 2. If we assume that the Tank 3 oxygen mechanically pressurizes Tank 2 in a plug flow without intermixing, the flow rate out of Tank 3 to do this is:

$$\omega_3 = \frac{\rho_3}{\rho_2} \left(\frac{V_2}{C_2 \phi_2 \theta_2} \dot{p} - \frac{Q_{HLK2}}{\theta_2} \right) \qquad (D4)$$

where the variables are as defined previously and the subscripts designate Tanks 2 and 3. For example, in the pressurization cycle shown in Figure 18, Tank 3 contains 49%, Tank 2 92%, and $\dot{p} = 168 \frac{psi}{hr}$. Then

$$\omega_3 = \frac{32}{64}\left(\frac{4.76(168)}{0.61(8.7)(140)} - \frac{7}{140}\right) = 0.51 \frac{lb}{hr} .$$

Since the average flow during this period is indicated to be 1.28 lb/hr, the flow during heater operation is estimated as 1.79 lb/hr.

Each cycle was evaluated as above and the average values determined. The results for Apollo 14 are shown in Figure 4.

Two Fluid Calculations

The amount of fluid interacting with the heater during each heater cycle can be determined from the pressure and temperature data using Equations (13) and (15). This will be illustrated for 90% quantity.

At 90% quantity the bulk physical properties are: $\rho_B = 63.95$ lb/ft^3, $C = 0.65$ (Figure 8), $\phi_B = 8.9$ psi ft^3/Btu and $\theta_B = 132$ Btu/lb (Figure 1), and $F(\rho_B) = 95.9$ Btu/lb (Figure 9). The variable K_B (Equation 14) is then:

$$K_B = \rho_B \theta_B \frac{C\phi_B}{V_T} = 63.95\ (132)\ \frac{(0.65)(8.9)}{4.76} = 10{,}200 \frac{psi}{ft^3} .$$

From Figure 3 the mean pressurization time for the 90% data is roughly 3.0 minutes. Since three heater elements are used at 90%, the heater energy rate into the fluid is:

$$Q_{HTR} = Q_{ELEC} - Q_{STOR} = 375 - 70 = 305 \frac{Btu}{hr}$$

where Q_{ELEC} is 125 $\frac{Btu}{hr}$ for each heater element and Q_{STOR} is determined as in Section D1. The total energy rate into the fluid is as given by Equation (C11)

$$Q_T = Q_{HTR} + Q_{HLK} - \Theta_B \omega_0$$

$$= 305 + 28 - 132\ (.85) = 221\ \text{Btu/hr}$$

where Q_{HLK} is given in Figure 19 and 0.85 lb/hr is the basic flow rate at 90% except during CM pressurization. The net energy into the fluid during each heater cycle at 90% is then:

$$\Delta Q \equiv Q_T \Delta t = 221\ (\frac{3.0}{60}) = 11.0\ \text{Btu}\ . \qquad \text{(D5)}$$

Equations (13) and (15) can be rearranged into the following more convenient forms:

$$V_S - V_S{}^I = \frac{\Delta P}{K_B} \qquad \text{(D6)}$$

and

$$m_S = \frac{\Delta Q}{F(\rho_B) - F(\rho_S)} \qquad \text{(D7)}$$

where $V_S - V_S{}^I$ can be equivalently expressed as

$$V_S - V_S{}^I = m_S (\frac{1}{\rho_S} - \frac{1}{\rho_B})\ . \qquad \text{(D8)}$$

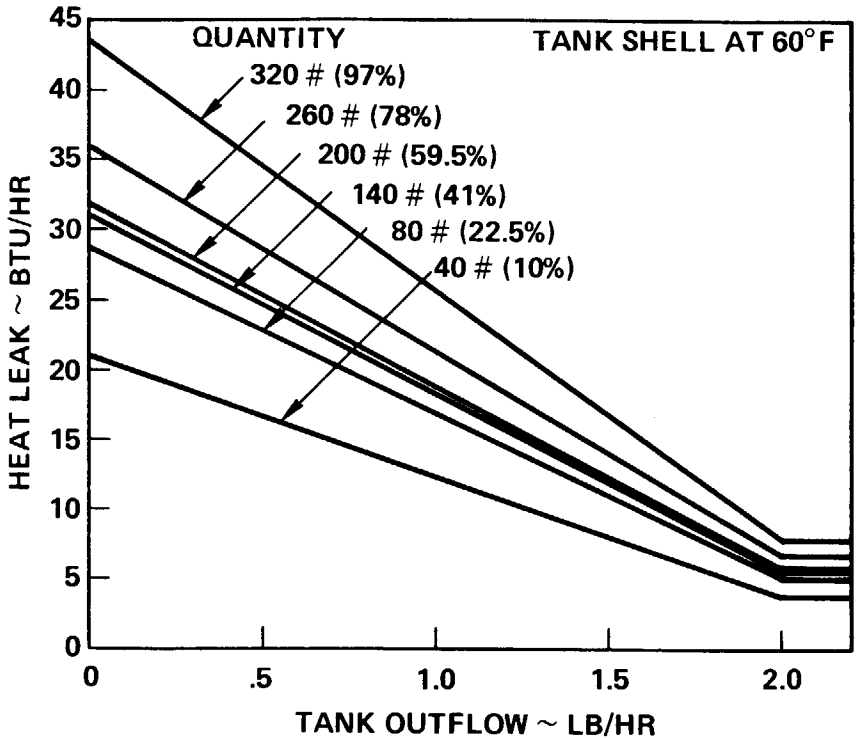

FIGURE 19 - OXYGEN TANK HEAT LEAK

Combining Equations (D6), (D7), and (D8) we get:

$$\frac{1}{\rho_S} + \frac{\Delta P}{K_B \Delta Q} F(\rho_S) = \frac{1}{\rho_B} + \frac{\Delta P}{K_B \Delta Q} F(\rho_B) \qquad \text{(D9)}$$

Substituting the values for 90%:

$$\frac{\Delta P}{K_B \Delta Q} = \frac{40}{(10{,}200)(11.0)} = 3.64 \times 10^{-4} \frac{ft^3}{Btu}$$

and

$$\frac{1}{\rho_S} + 3.64 \times 10^{-4} F(\rho_S) = \frac{1}{63.95} + 3.64 \times 10^{-4} (95.9) = .0505 \frac{ft^3}{lb}$$

The latter expression is solved by trial and error to yield:

$$\rho_S = 29.2 \frac{lb}{ft^3}$$

Then

$$F(\rho_S) = 44.8 \frac{Btu}{lb}$$

which when substituted into Equation (D7) gives

$$m_S = \frac{11.0}{95.9 - 44.8} = 0.214 \text{ lb} \quad .$$

The volume percent of the fluid contained within the bubble is then

$$\frac{V_S}{V_T}(100) = \frac{m_S(100)}{\rho_B V_T} = \frac{0.214\ (100)}{63.95\ (4.76)} = 0.07\% \qquad \text{(C10)}$$

The stratified volumes for other tank quantities have been computed in a similar manner. The results are shown in Figure 12.